Global dynamics in Einstein-Gauss-Bonnet scalar field cosmology with matter

Alfredo D. Millano,[1,*] Genly Leon,[1,2,†] and Andronikos Paliathanasis[2,1,‡]

[1]*Departamento de Matemáticas, Universidad Católica del Norte, Avenida Angamos 0610, Casilla 1280 Antofagasta, Chile*

[2]*Institute of Systems Science, Durban University of Technology, PO Box 1334, Durban 4000, South Africa*

(Received 23 April 2023; accepted 30 June 2023; published 20 July 2023)

We study the dynamics of the field equations in a four-dimensional isotropic and homogeneous spatially flat Friedmann-Lemaître-Robertson-Walker geometry in the context of Einstein-Gauss-Bonnet theory with a matter source and a scalar field coupled to the Gauss-Bonnet scalar. In this theory, the Gauss-Bonnet term contributes to the field equations. The mass of the scalar field depends on the potential function and the Gauss-Bonnet term. For the scalar field potential, we consider the exponential function and the coupling function between the scalar field and the Gauss-Bonnet scalar is considered to be the linear function. Moreover, the scalar field can have a phantom behavior. We consider a set of dimensionless variables and write the field equations into a system or algebraic-differential equations. For the latter, we investigate the equilibrium points and their stability properties. We use compactified variables to perform a global analysis of the asymptotic dynamics. This gravitational theory can explain the Universe's recent and past acceleration phases. Therefore, it can be used as a toy model for studying inflation or as a dark energy candidate.

DOI: 10.1103/PhysRevD.108.023519

I. INTRODUCTION

In the theory of general relativity, the physical space is described by a four-dimensional Riemannian manifold [1], and Ricci's scalar of the Levi-Civita connection expresses the Lagrangian of the field equations. In [2], it has been shown that the Einstein-Hilbert action integral of general relativity generated by Ricci's scalar with or without the cosmological constant term is the unique Action which gives second-order field equations in a four-dimensional manifold. That is not true in higher-order theories, where in [3], the most generic action integral was presented, providing second-order differential equations in an arbitrary dimensional spacetime. The so-called Lovelock gravity is the natural extension of general relativity.

General relativity is a well-tested theory for the description of astrophysical phenomena [4] and compact objects [5,6]; nevertheless, general relativity fails to explain the observational phenomena in cosmological scales. The cosmological observations indicate that the Universe at present is under an acceleration phase known as late-time acceleration [7,8]. However, it was proposed that the Universe had been under a previous acceleration phase in its very early stages. The inflationary mechanism can solve various observational phenomena such as the horizon problem, the flatness problem, the homogeneity of the Universe and other observations [9,10].

For the description of inflation, a scalar field is introduced in gravitational theory; in the slow-roll limit, the scalar field potential dominates the cosmological fluid drives acceleration dynamics to occur [11]. Furthermore, scalar fields have been introduced as dark energy candidates for the description of the late-time acceleration, see for instance [12–19] and references therein. Besides, scalar fields can attribute the degrees of freedom provided in the field equations from the introduction of geometric invariants during the modification of the Einstein-Hilbert action integral [20]. There is a taxonomy of modified theories of gravity proposed in the literature, which is divided into DE models linked to a fluid with the capability of accelerating the Universe and models in which the Einstein field equations of the general theory of relativity are modified; see the review articles [21–23].

Gauss-Bonnet gravity belongs to the family of Lovelock's theory, where the Gauss-Bonnet scalar is introduced in the action integral [24–28]. Compared to other modified gravity theories, some review of such theory is given in [29], and recently, was studied the cosmology of such theory concerning GWs [30–33].

The Gauss-Bonnet scalar is a topological invariant in a four-dimensional manifold, meaning it does not provide any terms in the field equations. In [34], to overpass this problem, the authors introduced a re-scale on the Gauss-Bonnet coupling constant such that a singular limit is introduced in Lovelock's gravity in the limit of the four

*alfredo.millano@alumnos.ucn.cl
†genly.leon@ucn.cl
‡anpaliat@phys.uoa.gr

dimensions (see, however, comment on this work in [35]). With the latter, the Gauss-Bonnet term introduces nontrivial terms to gravitational dynamics, and the field equations remain free from Ostrogradsky instabilities. The introduction of a nonlinear function of the Gauss-Bonnet scalar is another attempt to introduce nontrivial dynamical terms in the field equations in four-dimensional gravity [36–39]. Interestingly, in [37] was presented the possibility of eternal universes in Gauss-Bonnet theories of gravity in four dimensions for zero spatial curvature and a constraint over the derivative of the coupling function. Moreover, when the spatial curvature is present, they proposed generic results about the nature of the singularities. The authors generalized [40].

In this work, we are interested in the Einstein-Gauss-Bonnet scalar field gravity, where a scalar field coupled to the Gauss-Bonnet term is introduced in the gravitational action integral. The coupling function ensures that the Gauss-Bonnet term survives during the variation and affects the gravitational dynamics. In this theory, the mass of the scalar field depends on the Gauss-Bonnet component. The theory has been studied in cosmological scales [37,41,42] and astrophysical objects [31,43]. In the limit of a spatially flat Friedmann-Lemaître-Robertson-Walker (FLRW) the phase-space analysis for the field equations performed in [44–46]. It was found that the only equilibrium point where the Gauss-Bonnet term contributes to the cosmological fluid is that of the de Sitter universe. Nevertheless, in [47], a systematic analysis of the phase-space was presented where it was found that the new scaling solutions are supported in the Einstein-Gauss-Bonnet scalar theory, where the Gauss-Bonnet term contributes to the cosmological fluid. In the following, we extend the analysis presented in [47], where we introduce an ideal gas in the field equations. The latter is necessary to investigate if the Einstein-Gauss-Bonnet scalar theory can reproduce the cosmological history and to infer the theory's viability.

Interestingly, the model by [48,49] has no inflaton potential, but the inflaton couples to the Gauss-Bonnet term. In the case of quadratic coupling, they find inflation occurs with a graceful exit. Moreover, in [50], gradient instability exists in the tensor perturbations in this inflationary model. They further prove the no-go theorem for the Gauss-Bonnet inflation without an inflaton potential was proven.

The dynamical analysis of the gravitational field equations is a powerful method for the analysis of the asymptotic dynamics of the theory [51,52]. Gravity is a nonlinear theory, and even in cosmological studies where the field equations are ordinary differential equations, exact and analytic solutions are challenging to be found. Moreover, we can study asymptotic solutions' existence conditions and stability properties by analyzing the dynamics. Thus, we can solve the initial value problem and reconstruct the cosmological evolution and history [47,53]. The method has been widely applied in various gravitational models in cosmological studies [46,54–69] and for analyzing compact objects [70,71].

The structure of the paper is as follows. In Sec. II, the gravitational theory of our consideration, which is that of the four-dimensional Einstein-Gauss-Bonnet theory with a scalar field coupled to the Gauss-Bonnet term is presented. We consider a quintessence and a phantom scalar field. In Sec. III, we perform a detailed analysis of the phase-space for the exponential scalar field potential $V(\phi) = V_0 e^{\lambda\phi}$ and the linear coupling function $f(\phi) = f_0\phi$. In Sec. IV, we consider the case where the scalar field is massless. Section V studies the case where the model has no scalar field potential. Finally, we summarize our results in Sec. VI.

II. EINSTEIN-GAUSS-BONNET SCALAR FIELD 4D COSMOLOGY WITH MATTER

The gravitational theory of our consideration is that of the four-dimensional Einstein-Gauss-Bonnet theory with a scalar field coupled to the Gauss-Bonnet term. Hence, the gravitational action integral reads [38]

$$S = \int d^4x\sqrt{-g}\left(\frac{R}{2} - \frac{\varepsilon}{2}g_{\mu\nu}\phi^{;\mu}\phi^{;\nu} - V(\phi) - f(\phi)G + L_{\text{matter}}\right), \tag{1}$$

where R is the Ricci scalar of the metric tensor $g_{\mu\nu}$, ϕ is the scalar field, which inherits the symmetries of the background space, parameter ε takes the values $\varepsilon = \pm 1$ indicates if the scalar field ϕ is quintessence $(\varepsilon = +1)$ or phantom $(\varepsilon = -1)$, $V(\phi)$ is the scalar field potential, G is the Gauss-Bonnet term, $f(\phi)$ is the coupling function, which is considered to be a nonconstant and L_{matter} is the Lagrangian for the matter source. For an ideal gas with energy density ρ_m, the latter Lagrangian reads $L_{\text{matter}} = -\rho_m$.

For a spatially flat Friedmann-Lemaître-Robertson-Walker (FLRW) geometry with scale factor $a(t)$ and line element

$$ds^2 = -dt^2 + a^2(t)(dr^2 + r^2(d\theta^2 + \sin^2\theta d\varphi^2)), \tag{2}$$

the Ricci scalar and the Gauss-Bonnet scalars are

$$R = 6(2H^2 + \dot{H}), \tag{3}$$

and

$$G = 24H^2(\dot{H} + H^2). \tag{4}$$

in which $H = \frac{\dot{a}}{a}$ is the Hubble function, where a dot means derivative with respect to the independent variable t, that is $\dot{a} = \frac{da}{dt}$.

Thus, from the action integral (1) we can write the point-like Lagrangian for the field equations

$$L(a,\dot{a},\phi,\dot{\phi}) = -3a\dot{a}^2 + \frac{\varepsilon}{2}a^3\dot{\phi}^2 + 8\dot{a}^3 f_{,\phi}\dot{\phi} - a^3V(\phi) - a^3\rho_m, \tag{5}$$

where for the matter source it holds

$$\dot{\rho}_m + 3H(\rho_m + p_m) = 0, \tag{6}$$

in which p_m is the pressure for the matter source. Hence, for a constant equation of state parameter, i.e. $p_m = w_m\rho_m$, it follows

$$\rho_m = \rho_0 a^{-3(1+w_m)}, \tag{7}$$

from where it follows that (5) reads [38]

$$L(a,\dot{a},\phi,\dot{\phi}) = -3a\dot{a}^2 + \frac{\varepsilon}{2}a^3\dot{\phi}^2 + 8\dot{a}^3 f_{,\phi}\dot{\phi} - a^3V(\phi) - \rho_0 a^{-3w_m}. \tag{8}$$

For $f_{,\phi} = 0$, the latter Lagrangian function describes the scalar field theory without the Gauss-Bonnet term. Indeed in a four-dimensional spacetime, the Gauss-Bonnet term is a total derivative, and its contribution to the Euler-Lagrange equation is eliminated.

The gravitational field equations follow from the variation of the latter Lagrangian with respect to the dynamical variables $\{a,\phi\}$, while the constraint equation is the Hamiltonian function.

Indeed, the field equations are

$$-48H^3\dot{\phi}f'(\phi)^2 - 2\rho_m - 2V(\phi) - \epsilon\dot{\phi}^2 = 0, \tag{9}$$

$$-16H\dot{H}\dot{\phi}f'(\phi)^3\dot{\phi}f'(\phi) + \frac{1}{2}\epsilon\dot{\phi}^2 - V(\phi) + w_m\rho_m + H^2(-8\dot{\phi}^2 f''(\phi) - 8\ddot{\phi}f'(\phi) + 3) + 2\dot{H} = 0, \tag{10}$$

$$3H(-8H(\dot{H}+H^2)f'(\phi) - \epsilon\dot{\phi}) - V'(\phi) - \epsilon\ddot{\phi} = 0. \tag{11}$$

The effective density and pressure of the scalar field are given by

$$\rho_\phi = \frac{1}{2}\dot{\phi}(48H^3f'(\phi) + \epsilon\dot{\phi}) + V(\phi), \tag{12}$$

$$p_\phi = \frac{8H^2f'(\phi)V'(\phi)}{-8\epsilon H\dot{\phi}f'(\phi)^4f'(\phi)^2+\epsilon} - \frac{\epsilon V(\phi)}{-8\epsilon H\dot{\phi}f'(\phi)^4f'(\phi)^2+\epsilon} + \frac{192H^6f'(\phi)^2 + \epsilon\dot{\phi}(16H^2(\dot{\phi}f''(\phi) - 4Hf'(\phi)) - \epsilon\dot{\phi})}{16\epsilon H\dot{\phi}f'(\phi) - 2(96H^4f'(\phi)^2+\epsilon)}, \tag{13}$$

where we can define the effective equation of state (EoS) $\omega_\phi = \frac{p_\phi}{\rho_\phi}$.

In the following, we shall perform a detailed analysis of the phase-space for the exponential scalar field potential $V(\phi) = V_0e^{\lambda\phi}$ and the linear coupling function $f(\phi) = f_0\phi$.

III. LINEAR COUPLING

The field equations (9)–(11) become

$$-48f_0H^3\dot{\phi} + 6H^2 - 2\rho_m - 2V(\phi) - \epsilon\dot{\phi}^2 = 0, \tag{14}$$

$$-16f_0H\dot{H}\dot{\phi} + H^2(3 - 8f_0\ddot{\phi}) - 16f_0H^3\dot{\phi} + 2\dot{H} - V(\phi) + w_m\rho_m + \frac{1}{2}\epsilon\dot{\phi}^2 = 0, \tag{15}$$

$$-3H(8f_0H(\dot{H}+H^2) + \epsilon\dot{\phi}) - V'(\phi) - \epsilon\ddot{\phi} = 0. \tag{16}$$

together with the Eq. (6).

A. Dynamical system in dimensionless variables

To study the phase space, we introduce the following normalized dimensionless variables,

$$x = \frac{\phi'}{\sqrt{6}\sqrt{H^2+1}}, \qquad y = \frac{\sqrt{V(\phi)}}{\sqrt{3}\sqrt{H^2+1}}, \qquad z = \frac{\rho_m}{3(H^2+1)}, \qquad \eta = \frac{H}{\sqrt{1+H^2}}. \tag{17}$$

With these definitions, the first modified Friedmann equation is written in the algebraic form as

$$6(\eta^2-1)(-\eta^2 + \epsilon x^2 + y^2 + z) - 48\sqrt{6}f_0\eta^3x = 0. \tag{18}$$

Using Eq. (18) we can find the following definition for z

$$z = \frac{8\sqrt{6}f_0\eta^3x}{\eta^2-1} + \eta^2 - \epsilon x^2 - y^2. \tag{19}$$

Observe that when $x = y = 0$, we acquire $z = \eta^2$, which means $\Omega_m = \rho_m/(3H^2) = z/\eta^2 = 1$, and we have matter-dominated solutions.

By combining (17) and (19) we can write system (15) and (16) as follows

$$\frac{dx}{d\tau} = \frac{1}{K}[\eta(192f_0^2\eta^4x(\eta^2-3w_m) + 4\sqrt{6}f_0(\eta^2-1)\eta(\eta^2(2(3w_m-1)\epsilon x^2 - 3w_m - 1) + 3(w_m-5)\epsilon x^2)) - (\eta^2-1)y^2(\sqrt{6}(\eta^2(\lambda - 12f_0(w_m+1)) - \lambda) + 3\eta x(16f_0\lambda + \eta^2(8f_0\lambda + w_m\epsilon + \epsilon) - (w_m+1)\epsilon)) + \eta(3\epsilon(\eta^2-1)^2x((w_m+1)\eta^2 + x^2(\epsilon - w_m\epsilon) - 2))], \tag{20}$$

$$\frac{dy}{d\tau}=\frac{y}{4K}\left[384f_0^2\eta^7+6\epsilon(\eta^2-1)^2\eta\left(\frac{8\sqrt{6}f_0w_m\eta^3x}{\eta^2-1}+x^2(\epsilon-w_m\epsilon)-(w_m+1)(y^2-\eta^2)\right)\right.$$
$$\left.-16f_0(\eta^2-1)\eta^3(\sqrt{6}\epsilon\eta x+3\lambda y^2)+2\sqrt{6}\lambda x\right], \tag{21}$$

$$\frac{d\eta}{d\tau}=\frac{1}{K}\left[(\eta^2-1)\left(192f_0^2\eta^6+3\epsilon(\eta^2-1)^2\left(\frac{8\sqrt{6}f_0w_m\eta^3x}{\eta^2-1}+x^2(\epsilon-w_m\epsilon)-(w_m+1)(y^2-\eta^2)\right)\right)\right.$$
$$\left.+(-8f_0(\eta^2-1)^2\eta^2(\sqrt{6}\epsilon\eta x+3\lambda 8y^2))\right], \tag{22}$$

where we defined $K:=K(x,y,\eta,\epsilon,f_0)=192f_0^2\eta^4+2\epsilon(\eta^2-1)(8\sqrt{6}f_0\eta x+\eta^2-1)$ and introduce the time derivative $df/d\tau=1/\sqrt{1+H^2}df/dt$. We will also consider $-1\le\eta\le 1$ and $0\le w_m\le 1$.

B. General case for $\epsilon=1$

The equilibrium points for system (20)–(22) for $\epsilon=1$ in the coordinates (x,y,η) are the following:

(1) $M=(0,0,0)$, with eigenvalues $\{0,0,0\}$. The asymptotic solution is that of the Minkowski spacetime.

(2) $P_{1,2}=(0,0,\pm1)$, with eigenvalues $\{\pm1,\pm2,\pm(1-3w_m)\}$. These points describe a universe dominated by the Gauss-Bonnet term, and they verify that $\omega_\phi=-\frac{1}{3}$ and $q=0$. These points are
(a) P_1 is a source (P_2 is a sink) for $0\le w_m<\frac{1}{3}$,
(b) saddles for $\frac{1}{3}<w_m\le 1$, and
(c) nonhyperbolic for $w_m=\frac{1}{3}$.

(3) $P_3=\left(0,\sqrt{\frac{\lambda}{\lambda-8f_0}},\sqrt{\frac{\lambda}{\lambda-8f_0}}\right)$. This point exists for $f_0=0$ and $\lambda\neq 0$ or $f_0<0$ and $\lambda\ge 0$ or $f_0>0$ and $\lambda\le 0$. The eigenvalues are $\left\{-\frac{3\sqrt{\lambda}(w_m+1)}{\sqrt{\lambda-8f_0}},-\frac{\sqrt{\lambda}(3\sqrt{3\lambda^2+2}+\sqrt{51\lambda^2+18})}{2\sqrt{3\lambda^2+2}\sqrt{\lambda-8f_0}},\frac{\sqrt{\lambda}(\sqrt{51\lambda^2+18}-3\sqrt{3\lambda^2+2})}{2\sqrt{3\lambda^2+2}\sqrt{\lambda-8f_0}}\right\}$. This point describes a de Sitter universe, and we verify that $\omega_\phi=-1$ and $q=-1$. We also verify that the point is a saddle.

(4) $P_4=\left(0,\sqrt{\frac{\lambda}{\lambda-8f_0}},-\sqrt{\frac{\lambda}{\lambda-8f_0}}\right)$, with eigenvalues $\left\{\frac{3\sqrt{\lambda}(w_m+1)}{\sqrt{\lambda-8f_0}},\frac{\sqrt{\lambda}(3\sqrt{3\lambda^2+2}-\sqrt{51\lambda^2+18})}{2\sqrt{3\lambda^2+2}\sqrt{\lambda-8f_0}},\frac{\sqrt{\lambda}(3\sqrt{3\lambda^2+2}+\sqrt{51\lambda^2+18})}{2\sqrt{3\lambda^2+2}\sqrt{\lambda-8f_0}}\right\}$. This point existence conditions, values for ω_ϕ,q, physical interpretation and stability are the same as P_3.

In Fig. 1 we present the stability analysis for system (20)–(22) with $\epsilon=1$ and different values of the parameters λ and f_0. We consider $y>0$; however, the system is unbounded, suggesting nontrivial dynamics at infinity. We also considered the three cases $w_m=0$ (dust), $\frac{1}{3}$ (radiation) and 1 (stiff matter). A summary of the results of this section is presented in Table I.

Figure 2 displays the expressions $\omega_\phi(\tau)$, $x(\tau)$, $y(\tau)$, and $\eta(\tau)$ evaluated at a solution of system (20)–(22) for $\epsilon=1$ for the initial conditions for the left plot are $x(0)=0.001, y(0)=\sqrt{\frac{\lambda}{\lambda-8f_0}},\eta(0)=-\sqrt{\frac{\lambda}{\lambda-8f_0}}$ (i.e., near the saddle point P_3). The solution is past asymptotic to $\omega_\phi=-1$ ($q=-1$), then remains near the de Sitter point P_3, then tending asymptotically to $\omega_\phi=-\frac{1}{3}$ (the Gauss-Bonnet

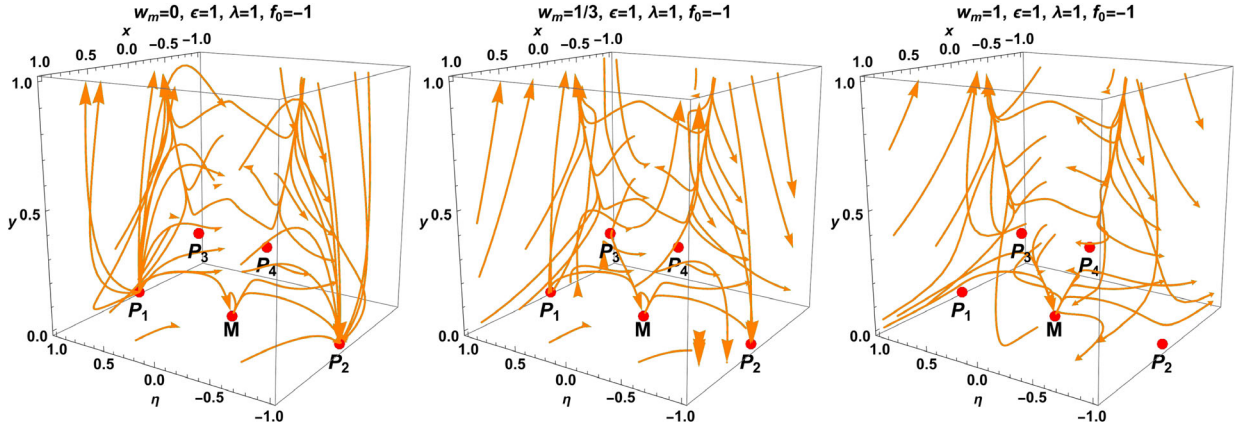

FIG. 1. Phase-space analysis for system (20)–(22) for $\epsilon=1$ and different values of the parameters λ, f_0. Here we consider $Y>0$ and the three cases $w_m=0,\frac{1}{3},1$.

TABLE I. Equilibrium points of system (20)–(22) for $\epsilon = 1$ with their stability conditions. Also includes the value of ω_ϕ and q.

Label	x	y	η	Stability	ω_ϕ	q
M	0	0	0	Nonhyperbolic	Indeterminate	Indeterminate
P_1	0	0	1	Source for $0 \le w_m < 1/3$ Saddle for $1/3 < w_m \le 1$ Nonhyperbolic for $w_m = 1/3$	$-\frac{1}{3}$	0
P_2	0	0	-1	Sink for $0 \le w_m < 1/3$ Saddle for $1/3 < w_m \le 1$ Nonhyperbolic for $w_m = 1/3$	$-\frac{1}{3}$	0
P_3	0	$\sqrt{\frac{\lambda}{\lambda-8f_0}}$	$\sqrt{\frac{\lambda}{\lambda-8f_0}}$	Saddle	-1	-1
P_4	0	$\sqrt{\frac{\lambda}{\lambda-8f_0}}$	$-\sqrt{\frac{\lambda}{\lambda-8f_0}}$	Saddle	-1	-1

point P_2) from below. The initial conditions for the plot on the right are $x(0) = 0.001, y(0) = 0.001, \eta(0) = 0.9$ (i.e., near the source point P_1). The solution is past asymptotic to $\omega_\phi = -\frac{1}{3}, q = 0$ (zero acceleration), then it grows to $\omega_\phi, q > 0$, finally, it tends asymptotically to $\omega_\phi = 0, q = \frac{1}{2}$ describing a matter-dominated solution.

C. General case for $\epsilon = -1$

The equilibrium points for system (20)–(22) are the same as in Sec. III B plus some additional points, the complete list of equilibrium points in the coordinates (x, y, η) is the following.

(1) $M = (0, 0, 0)$. The stability analysis and physical interpretation are the same as in Sec. III B.

(2) $P_{1,2} = (0, 0, \pm 1)$. The stability analysis and physical interpretation are the same as in Sec. III B.

(3) $P_3 = \left(0, \sqrt{\frac{\lambda}{\lambda-8f_0}}, \sqrt{\frac{\lambda}{\lambda-8f_0}}\right)$. The existence conditions and physical interpretation are the same as in the Sec. III B; however, the second and third eigenvalues slightly change to $\left\{-\frac{3\sqrt{\lambda}(w_m+1)}{\sqrt{\lambda-8f0}}, -\frac{\sqrt{\lambda}(3\sqrt{3\lambda^2-2}+\sqrt{51\lambda^2-18})}{2\sqrt{3\lambda^2-2}\sqrt{\lambda-8f0}}, \frac{\sqrt{\lambda}(\sqrt{51\lambda^2-18}-3\sqrt{3\lambda^2-2})}{2\sqrt{3\lambda^2-2}\sqrt{\lambda-8f0}}\right\}$, therefore the stability changes to

(a) a sink for
  (i) $f_0 < 0, 0 < \lambda < \sqrt{\frac{2}{3}}$ or
  (ii) $f_0 > 0, -\sqrt{\frac{2}{3}} < \lambda < 0$,

(b) a saddle for
  (i) $f_0 < 0, \lambda > \sqrt{\frac{2}{3}}$ or
  (ii) $f_0 > 0, \lambda < -\sqrt{\frac{2}{3}}$.

(4) $P_4 = \left(0, \sqrt{\frac{\lambda}{\lambda-8f_0}}, -\sqrt{\frac{\lambda}{\lambda-8f_0}}\right)$. The existence conditions and physical interpretation are the same as in the Sec. III B however, the second and third eigenvalues slightly change to $\left\{\frac{3\sqrt{\lambda}(w_m+1)}{\sqrt{\lambda-8f0}}, \frac{\sqrt{\lambda}(3\sqrt{3\lambda^2-2}-\sqrt{51\lambda^2-18})}{2\sqrt{3\lambda^2-2}\sqrt{\lambda-8f0}}, \frac{\sqrt{\lambda}(3\sqrt{3\lambda^2-2}+\sqrt{51\lambda^2-18})}{2\sqrt{3\lambda^2-2}\sqrt{\lambda-8f0}}\right\}$, therefore the stability changes to

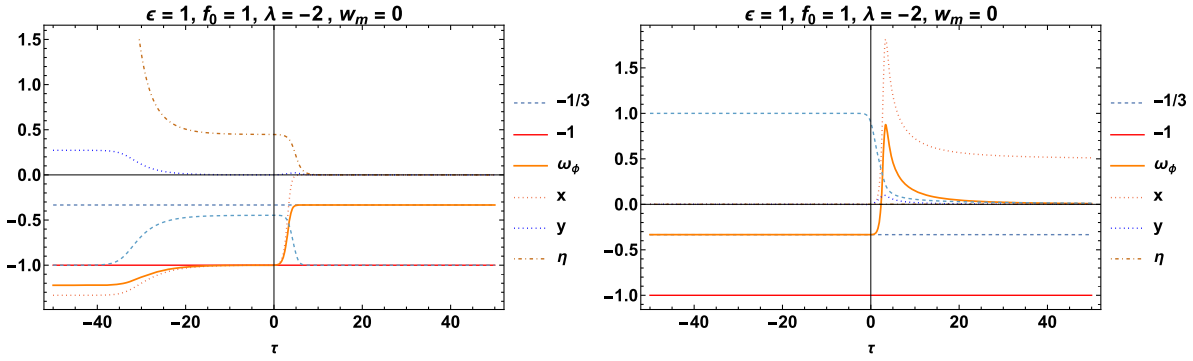

FIG. 2. $\omega_\phi(\tau)$, $x(\tau)$, $y(\tau)$, and $\eta(\tau)$ evaluated at a solution of system (20)–(22) for $\epsilon = 1$. The initial conditions for the left plot are $x(0) = 0.001, y(0) = \sqrt{\frac{\lambda}{\lambda-8f_0}}, \eta(0) = -\sqrt{\frac{\lambda}{\lambda-8f_0}}$ (i.e., near the saddle point P_3). The solution is past asymptotic to $\omega_\phi = -1$ ($q = -1$), then remains near the de Sitter point P_3, then tending asymptotically to $\omega_\phi = -\frac{1}{3}$ (the Gauss-Bonnet point P_2) from below. The initial conditions for the plot on the right are $x(0) = 0.001, y(0) = 0.001, \eta(0) = 0.9$ (i.e., near the source point P_1). The solution is past asymptotic to $\omega_\phi = -\frac{1}{3}, q = 0$ (zero acceleration), then it grows to $\omega_\phi, q > 0$, finally, it tends asymptotically to $\omega_\phi = 0, q = \frac{1}{2}$ describing a matter-dominated solution.

(a) a source for
  (i) $f_0 < 0$, $0 < \lambda < \sqrt{\frac{2}{3}}$ or
  (ii) $f_0 > 0$, $-\sqrt{\frac{2}{3}} < \lambda < 0$,
(b) a saddle for
  (i) $f_0 < 0$, $\lambda > \sqrt{\frac{2}{3}}$ or
  (ii) $f_0 > 0$, $\lambda < -\sqrt{\frac{2}{3}}$.

(5) $P_5 = \left(\sqrt{\frac{1}{20\sqrt{\frac{10}{3}}f_0+5}}, 0, \sqrt{3}\sqrt{\frac{1}{4\sqrt{30}f_0+3}}\right)$, with eigenvalues $\left\{-\frac{3(w_m+1)}{\sqrt{4\sqrt{\frac{10}{3}}f_0+1}}, -\frac{9(4\sqrt{10}f_0+\sqrt{3})}{(4\sqrt{30}f_0+3)^{3/2}}, \frac{3\lambda}{\sqrt{40\sqrt{30}f_0+30}}\right\}$. This point exists for $f_0 \geq 0$, the asymptotic solution it describes is that of a de Sitter universe; also, we verify that $\omega_\phi = -1$ and $q = -1$. The stability conditions are
(a) a sink for $f_0 \geq 0$, $\lambda < 0$,
(b) a saddle for $f_0 \geq 0$, $\lambda > 0$, and
(c) nonhyperbolic for $f_0 \geq 0$, $\lambda = 0$.

(6) $P_6 = \left(-\sqrt{\frac{1}{20\sqrt{\frac{10}{3}}f_0+5}}, 0, -\sqrt{3}\sqrt{\frac{1}{4\sqrt{30}f_0+3}}\right)$, with eigenvalues $\left\{\frac{9(4\sqrt{10}f_0+\sqrt{3})}{(4\sqrt{30}f_0+3)^{3/2}}, \frac{3(w_m+1)}{\sqrt{4\sqrt{\frac{10}{3}}f_0+1}}, -\frac{3\lambda}{\sqrt{40\sqrt{30}f_0+30}}\right\}$. This point exists for $f_0 \geq 0$, the asymptotic solution it describes is that of a de Sitter universe; also, we verify that $\omega_\phi = -1$ and $q = -1$. The stability conditions are
(a) a source for $f_0 \geq 0$, $\lambda < 0$,
(b) a saddle for $f_0 \geq 0$, $\lambda > 0$, and
(c) nonhyperbolic for $f_0 \geq 0$, $\lambda = 0$.

(7) $P_7 = \left(\sqrt{\frac{1}{5-20\sqrt{\frac{10}{3}}f_0}}, 0, -\sqrt{3}\sqrt{\frac{1}{3-4\sqrt{30}f_0}}\right)$, with eigenvalues $\lambda_1 = \frac{3\lambda}{\sqrt{30-40\sqrt{30}f_0}}$ and $\lambda_{2,3}$ given by $\left\{\frac{9(\sqrt{(\sqrt{3}-4\sqrt{10}f_0)^2}w_m-4\sqrt{10}f_0(w_m+2)+\sqrt{3}(w_m+2))}{2(3-4\sqrt{30}f_0)^{3/2}}, -\frac{9\sqrt{(\sqrt{3}-4\sqrt{10}f_0)^2}w_m+36\sqrt{10}f_0(w_m+2)-9\sqrt{3}(w_m+2)}{2(3-4\sqrt{30}f_0)^{3/2}}\right\}$. This point exists for $f_0 \leq 0$, the asymptotic solution it describes is that of a de Sitter universe; also, we verify that $\omega_\phi = -1$ and $q = -1$. The stability conditions are
(a) a source for $f_0 \leq 0$, $\lambda > 0$,
(b) a saddle for $f_0 \leq 0$, $\lambda < 0$, and
(c) nonhyperbolic for $f_0 \leq 0$, $\lambda = 0$.

(8) $P_8 = \left(-\sqrt{\frac{1}{5-20\sqrt{\frac{10}{3}}f_0}}, 0, \sqrt{3}\sqrt{\frac{1}{3-4\sqrt{30}f_0}}\right)$, with eigenvalues $\lambda_1 = -\frac{3\lambda}{\sqrt{30-40\sqrt{30}f_0}}$ and $\lambda_{2,3}$ given by $\left\{\frac{9\sqrt{(\sqrt{3}-4\sqrt{10}f_0)^2}w_m+36\sqrt{10}f_0(w_m+2)-9\sqrt{3}(w_m+2)}{2(3-4\sqrt{30}f_0)^{3/2}}, -\frac{9(\sqrt{(\sqrt{3}-4\sqrt{10}f_0)^2}w_m-4\sqrt{10}f_0(w_m+2)+\sqrt{3}(w_m+2))}{2(3-4\sqrt{30}f_0)^{3/2}}\right\}$. This

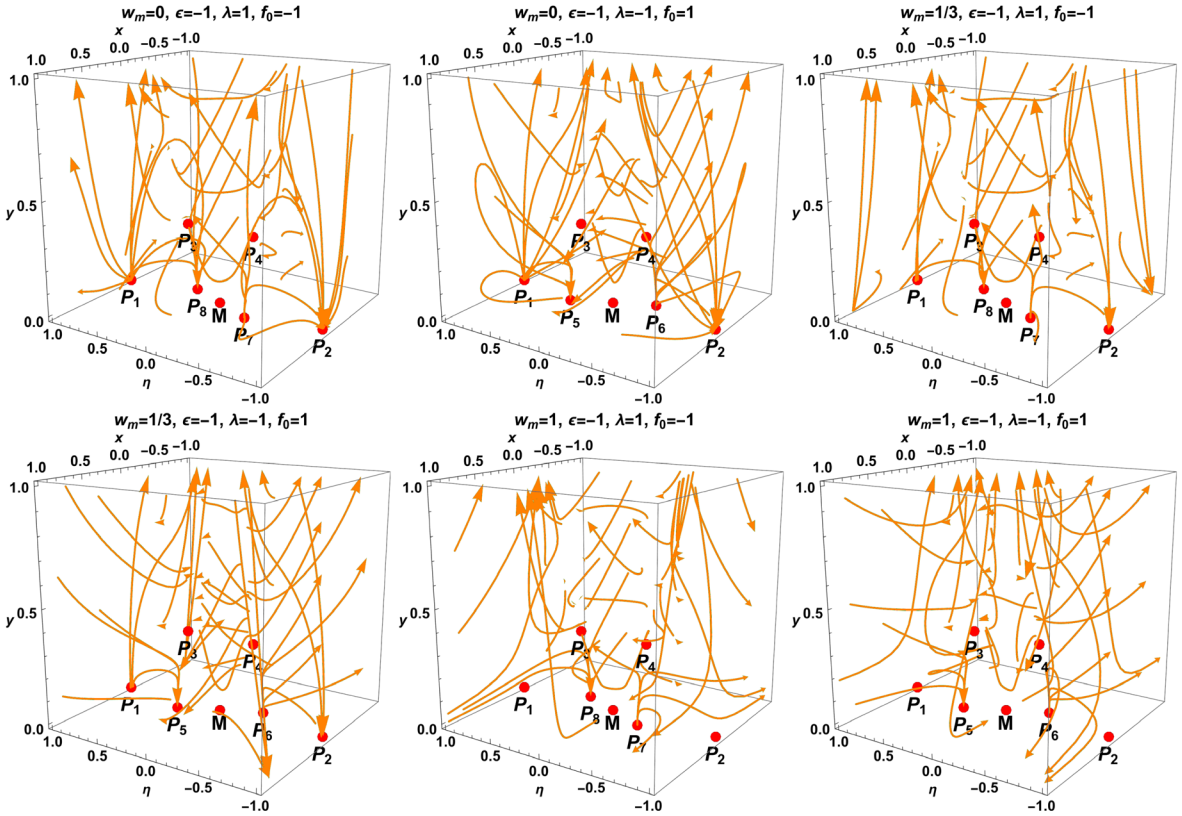

FIG. 3. Phase-space analysis for system (20)–(22) for $\epsilon = -1$ and different values of the parameters λ, f_0. Here we consider $Y > 0$ and the three cases $w_m = 0, \frac{1}{3}, 1$.

TABLE II. Equilibrium points of system (20)–(22) for $\epsilon = -1$ with their stability conditions. Also includes the value of ω_ϕ and q.

Label	x	y	η	Stability	ω_ϕ	q
M	0	0	0	Nonhyperbolic	Indeterminate	Indeterminate
P_1	0	0	1	Source for $0 \leq w_m < 1/3$		
				Saddle for $1/3 < w_m \leq 1$		
				Nonhyperbolic for $w_m = 1/3$	$-\frac{1}{3}$	0
P_2	0	0	-1	Sink for $0 \leq w_m < 1/3$		
				Saddle for $1/3 < w_m \leq 1$		
				Nonhyperbolic for $w_m = 1/3$	$-\frac{1}{3}$	0
P_3	0	$\sqrt{\frac{\lambda}{\lambda-8f_0}}$	$\sqrt{\frac{\lambda}{\lambda-8f_0}}$	Saddle	-1	-1
P_4	0	$\sqrt{\frac{\lambda}{\lambda-8f_0}}$	$-\sqrt{\frac{\lambda}{\lambda-8f_0}}$	Saddle	-1	-1
P_5	$\sqrt{\frac{1}{20\sqrt{\frac{10}{3}}f_0+5}}$	0	$\sqrt{3}\sqrt{\frac{1}{4\sqrt{30}f_0+3}}$	Sink for $f_0 \geq 0, \lambda < 0$		
				Saddle for $f_0 \geq 0, \lambda < 0$		
				Nonhyperbolic for $f_0 \geq 0, \lambda = 0$	-1	-1
P_6	$\sqrt{\frac{1}{20\sqrt{\frac{10}{3}}f_0+5}}$	0	$\sqrt{3}\sqrt{\frac{1}{4\sqrt{30}f_0+3}}$	Source for $f_0 \geq 0, \lambda < 0$		
				Saddle for $f_0 \geq 0, \lambda < 0$		
				Nonhyperbolic for $f_0 \geq 0, \lambda = 0$	-1	-1
P_7	$\sqrt{\frac{1}{5-20\sqrt{\frac{10}{3}}f_0}}$	0	$-\sqrt{3}\sqrt{\frac{1}{3-4\sqrt{30}f_0}}$	Source for $f_0 \leq 0, \lambda > 0$		
				Saddle for $f_0 \leq 0, \lambda < 0$		
				Nonhyperbolic for $f_0 \leq 0, \lambda = 0$	-1	-1
P_8	$-\sqrt{\frac{1}{5-20\sqrt{\frac{10}{3}}f_0}}$	0	$\sqrt{3}\sqrt{\frac{1}{3-4\sqrt{30}f_0}}$	Sink for $f_0 \leq 0, \lambda > 0$		
				Saddle for $f_0 \leq 0, \lambda < 0$		
				Nonhyperbolic for $f_0 \leq 0, \lambda = 0$	-1	-1

point exists for $f_0 \leq 0$, the asymptotic solution it describes is that of a de Sitter universe; also, we verify that $\omega_\phi = -1$ and $q = -1$. The stability conditions are

(a) a sink for $f_0 \leq 0$, $\lambda > 0$,
(b) a saddle for $f_0 \leq 0$, $\lambda < 0$, and
(c) nonhyperbolic for $f_0 \leq 0$, $\lambda = 0$.

In Fig. 3 we present the stability analysis for system (20)–(22) with $\epsilon = -1$ and different values of the parameters λ and f_0. We consider $y > 0$; however, the system is unbounded, suggesting nontrivial dynamics at infinity. We also considered the three cases $w_m = 0$ (dust), $\frac{1}{3}$ (radiation) and 1 (stiff matter). A summary of the results of this section is presented in Table II.

In Fig. 4 we present the expressions $\omega_\phi(\tau)$, $x(\tau)$, $y(\tau)$, and $\eta(\tau)$ evaluated at the solution of system (20)–(22) for $\epsilon = -1$. The initial conditions for the left plot are

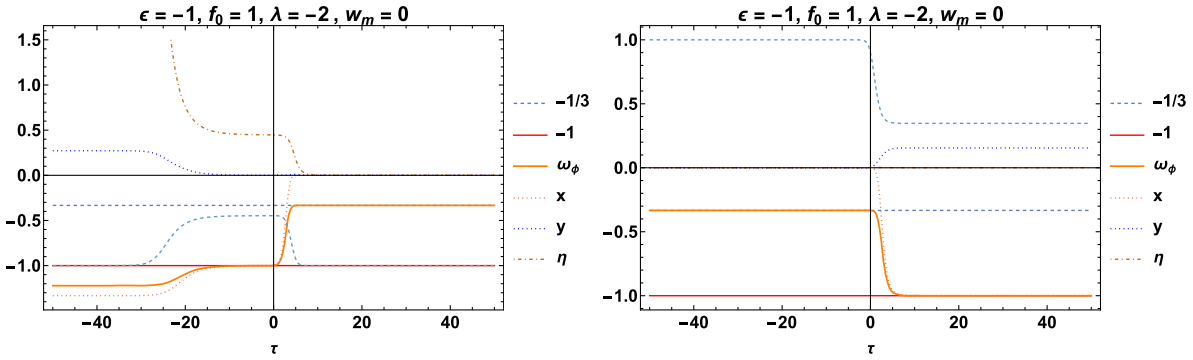

FIG. 4. $\omega_\phi(\tau)$, $x(\tau)$, $y(\tau)$, and $\eta(\tau)$ evaluated at the solution of system (20)–(22) for $\epsilon = -1$. The initial conditions for the left plot are $x(0) = 0.001, y(0) = \sqrt{\frac{\lambda}{\lambda-8f_0}}, \eta(0) = -\sqrt{\frac{\lambda}{\lambda-8f_0}}$ (i.e., near the saddle point P_3). The solution is past asymptotic to $\omega_\phi = -1$ ($q = -1$), then remains near the de Sitter point P_3, then tending asymptotically to $\omega_\phi = -\frac{1}{3}$ (the Gauss-Bonnet point P_2) from below. The initial conditions for the plot on the right are $x(0) = 0.001, y(0) = 0.001, \eta(0) = 0.9$ (i.e., near the source point P_1). The solution is past asymptotic to $\omega_\phi = -\frac{1}{3}$ (zero acceleration), then it tends asymptotically to a de Sitter phase $\omega_\phi = -1, q = -1$ describing a late-time acceleration.

$x(0) = 0.001, y(0) = \sqrt{\frac{\lambda}{\lambda-8f_0}}, \eta(0) = -\sqrt{\frac{\lambda}{\lambda-8f_0}}$ (i.e., near the saddle point P_3). The solution is past asymptotic to $\omega_\phi = -1$ ($q = -1$), then remains near the de Sitter point P_3, then tending asymptotically to $\omega_\phi = -\frac{1}{3}$ (the Gauss-Bonnet point P_2) from below. The initial conditions for the plot on the right are $x(0) = 0.001, y(0) = 0.001, \eta(0) = 0.9$ (i.e., near the source point P_1). The solution is past asymptotic to $\omega_\phi = -\frac{1}{3}$ (zero acceleration), then it tends asymptotically to a de Sitter phase $\omega_\phi = -1, q = -1$ describing a late-time acceleration.

IV. DYNAMICS AT INFINITY

As suggested before, we are interested in the behavior of the dynamical system at infinity; for that purpose, we define the new compact variables

$$X = \frac{x}{\sqrt{1+x^2+y^2}}, \qquad Y = \frac{y}{\sqrt{1+x^2+y^2}}, \tag{23}$$

and the new derivative

$$\frac{df}{ds} = Z\frac{df}{d\tau}, \qquad Z = \sqrt{1-X^2-Y^2}. \tag{24}$$

With these definitions, we obtain the following dynamical system

$$\begin{aligned}\frac{dX}{ds} = -\frac{1}{L}[&(\eta^2-1)(48f_0\lambda X\eta + \sqrt{6}Z((\lambda-12f_0(w_m+1))\eta^2-\lambda))Y^4\\
&+(48f_0\epsilon\lambda\eta(\eta^2-1)X^3+\sqrt{6}Z((96\lambda f_0^2-12(w_m-5)\epsilon f_0+\epsilon\lambda)\eta^4-2\epsilon(\lambda-6f_0(w_m-5))\eta^2+\epsilon\lambda)X^2\\
&+3Z^2\eta((192w_m f_0^2+8\lambda f_0+(w_m+3)\epsilon)\eta^4-2((w_m+3)\epsilon-4f_0\lambda)\eta^2+(w_m+3)\epsilon-16f_0\lambda)X\\
&+\sqrt{6}Z^3(\eta^2-1)(4(3w_m f_0+f_0)\eta^4+(\lambda-12f_0(w_m+1))\eta^2-\lambda))Y^2\\
&-Z^2\eta(-3(w_m-1)\epsilon^2(\eta^2-1)^2X^3+4\sqrt{6}f_0\epsilon Z\eta(\eta^2-1)((6w_m-2)\eta^2+3(w_m-5))X^2\\
&+3Z^2((64f_0^2+w_m\epsilon+\epsilon)\eta^6-2(96w_m f_0^2+(w_m+2)\epsilon)\eta^4+(w_m+5)\epsilon\eta^2-2\epsilon)X\\
&-4\sqrt{6}f_0(3w_m+1)Z^3\eta^3(\eta^2-1))],\end{aligned} \tag{25}$$

$$\begin{aligned}\frac{dY}{ds} = \frac{Y}{L}[&48f_0\epsilon\lambda\eta(\eta^2-1)X^4+\sqrt{6}Z((96\lambda f_0^2-12(w_m-5)\epsilon f_0+\epsilon\lambda)\eta^4-2\epsilon(\lambda-6f_0(w_m-5))\eta^2+\epsilon\lambda)X^3+3\eta(16f_0\lambda(\eta^2-1)Y^2\\
&+Z^2((192w_m f_0^2+\epsilon(-w_m\epsilon+\epsilon+2))\eta^4+2\epsilon((w_m-1)\epsilon+8f_0\lambda-2)\eta^2+\epsilon(-w_m\epsilon+\epsilon-16f_0\lambda+2)))X^2\\
&+\sqrt{6}Z((\eta^2-1)((\lambda-12f_0(w_m+1))\eta^2-\lambda)Y^2+Z^2(4f_0(-2\epsilon+w_m(6\epsilon+3)+1)\eta^6\\
&+(96\lambda f_0^2-4(6\epsilon w_m+3w_m-2\epsilon+1)f_0+\epsilon\lambda)\eta^4-2\epsilon\lambda\eta^2+\epsilon\lambda))X\\
&-3Y^2Z^2\eta(\eta^2-1)((w_m\epsilon+\epsilon+8f_0\lambda)\eta^2-(w_m+1)\epsilon)+3Z^4\eta^3((64f_0^2+w_m\epsilon+\epsilon)\eta^4-2(w_m+1)\epsilon\eta^2+(w_m+1)\epsilon)],\end{aligned} \tag{26}$$

$$\begin{aligned}\frac{d\eta}{ds} = \frac{(\eta^2-1)}{L}[&8\sqrt{6}f_0(3w_m-1)\epsilon XZ(\eta^2-1)\eta^3+3Z^2((64f_0^2+w_m\epsilon+\epsilon)\eta^4-2(w_m+1)\epsilon\eta^2+(w_m+1)\epsilon)\eta^2\\
&-3(w_m-1)\epsilon^2X^2(\eta^2-1)^2-3Y^2(\eta^2-1)((w_m\epsilon+\epsilon+8f_0\lambda)\eta^2-(w_m+1)\epsilon)],\end{aligned} \tag{27}$$

where

$$L = 2(8\sqrt{6}f_0\epsilon X\eta(\eta^2-1)+Z((96f_0^2+\epsilon)\eta^4-2\epsilon\eta^2+\epsilon)). \tag{28}$$

To obtain the equilibrium points at infinity, we define the cylindrical coordinates (ρ, θ, η)

$$X = \rho\cos(\theta), \qquad Y = \rho\sin(\theta), \quad \eta = \eta, \tag{29}$$

such that $X^2 + Y^2 \to 1$ corresponds to $\rho \to 1$.

Then, as $\rho \to 1$ we have the leading terms

$$\begin{aligned}\frac{d\rho}{ds} = -\frac{1}{8f_0\epsilon}\sqrt{\frac{3}{2}}(1-\rho)\cos(\theta)[&\eta^2(8f_0\lambda\tan^2(\theta)+\epsilon((w_m+1)\ \sec^2(\theta)+(w_m-1)\epsilon-w_m-1))\\
&-16f_0\lambda(\epsilon-1)\sin^2(\theta)+\epsilon(-((w_m+1)\ \sec^2(\theta))-w_m\epsilon+w_m+\epsilon+1)],\end{aligned} \tag{30}$$

$$\frac{d\theta}{ds}=\frac{\sqrt{\frac{3}{2}}\lambda\sin(\theta)((\epsilon-1)\cos(2\theta)+\epsilon+1)}{2\epsilon}, \tag{31}$$

$$\begin{aligned}\frac{d\eta}{ds}=&-\frac{\sqrt{\frac{3}{2}}(\eta^2-1)}{16f_0\epsilon\eta}[\eta^2(\sin(\theta)\tan(\theta)(8f_0\lambda+w_m\epsilon+\epsilon)\\&+(w_m-1)\epsilon^2\cos(\theta))-\epsilon((w_m+1)\sin(\theta)\tan(\theta)\\&+(w_m-1)\epsilon\cos(\theta))].\end{aligned} \tag{32}$$

A. Analysis at infinity for $\epsilon=1$

Recall that the equilibrium points for this case are the same ones as the finite regime in Sec. III B plus the following additional points described in this section. Since $Y>0$, we set $\theta\in[0,\pi]$. Therefore, the points at infinity for $\epsilon=+1$ in the coordinates (ρ,θ,η) are

(1) $Q_{1,2}=(1,0,\pm1)$, with eigenvalues $\{0,0,\sqrt{\frac{3}{2}}\lambda\}$. These points satisfy $\omega_\phi=-\frac{1}{3}$, $q=0$, this means that the points described a universe dominated by the Gauss-Bonnet term.

(2) $Q_{3,4}=(1,\pi,\pm1)$, with eigenvalues $\{0,0,-\sqrt{\frac{3}{2}}\lambda\}$. These points satisfy $\omega_\phi=-\frac{1}{3}$, $q=0$, the physical interpretation is the same as the previous points.

The third eigenvalue corresponds to the θ-axis. To analyze the nonhyperbolic nature of the critical points in the plane (ρ,η), we consider the variable τ as the independent variable. This is equivalent to divide the system (30)–(32) by $\sqrt{1-\rho^2}$.

The points $Q_{1,2}$ in the re-scaled system have the eigenspace given by

$$\begin{pmatrix}\pm2 & \pm2(3w_m-1) & \text{sign}(\lambda)\infty\\ \{0,0,1\} & \{1,0,0\} & \{0,1,0\}\end{pmatrix}. \tag{33}$$

For the points $Q_{3,4}$ in the rescaled system has the eigenspace given by

$$\begin{pmatrix}\pm2 & \pm2(3w_m-1) & -\text{sign}(\lambda)\infty\\ \{0,0,1\} & \{1,0,0\} & \{0,1,0\}\end{pmatrix}. \tag{34}$$

The last column with infinity entries is an artefact of the division by $\sqrt{1-\rho^2}$ as $\rho\to1$. Therefore, by combining the two approaches, we obtain that,

(1) $Q_{1,2}$ with eigenvalues $\{\pm2,\pm2(3w_m-1),\sqrt{\frac{3}{2}}\lambda\}$ satisfy the following
   (a) Q_1 is a source (Q_2 is a sink) for $\lambda>0$, $\frac{1}{3}<w_m\leq1$.
   (b) They are saddles for
      (i) $\lambda\neq0$, $0\leq w_m<\frac{1}{3}$,
      (ii) $\lambda<0$, $\frac{1}{3}<w_m\leq1$.
   (c) Nonhyperbolic for $\lambda=0$ or $w_m=\frac{1}{3}$.

(2) $Q_{3,4}$ with eigenvalues $\{\pm2,\pm2(3w_m-1),-\sqrt{\frac{3}{2}}\lambda\}$ satisfy the following.
   (a) Q_3 is a source (Q_4 is a sink) for $\lambda<0$, $\frac{1}{3}<w_m\leq1$.
   (b) They are saddles for
      (i) $\lambda\neq0$, $0\leq w_m<\frac{1}{3}$,
      (ii) $\lambda>0$, $\frac{1}{3}<w_m\leq1$.
   (c) They are nonhyperbolic for $\lambda=0$ or $w_m=\frac{1}{3}$.

In Fig. 5 we present the phase-space analysis for system (25)–(27) for $\epsilon=1$ and different values of the parameters λ,f_0. Where we defined the region $0\leq X^2+Y^2\leq1$, $Y>0$ and $-1\leq\eta\leq1$ defining half a cylinder. We also considered the three cases $w_m=0$ (dust), $\frac{1}{3}$ (radiation), and 1 (stiff matter).

B. Analysis at infinity for $\epsilon=-1$

As in the previous section, we consider $\theta\in[0,\pi]$. The equilibrium points for this case are the same ones from Sec. III C plus the following the points at infinity for $\epsilon=-1$ in the coordinates (ρ,θ,η), say,

(1) $Q_{1,2}=(1,0,\pm1)$, with eigenvalues $\{0,0,\sqrt{\frac{2}{3}}\lambda\}$. These points verify that $\omega_\phi=-\frac{1}{3}$ and $q=0$. These points describe a universe dominated by the Gauss-Bonnet term, and the analysis is the same as in Sec. IV A.

(2) $Q_{3,4}=(1,\pi,\pm1)$, with eigenvalues $\{0,0,\sqrt{\frac{2}{3}}\lambda\}$. These points verify that $\omega_\phi=-\frac{1}{3}$ and $q=0$. These points describe a universe dominated by the Gauss-Bonnet term, and the analysis is the same as in Sec. IV A.

(3) $Q_{5,6}=(1,\frac{\pi}{4},\pm1)$, with eigenvalues $\{0,-\frac{\sqrt{3}\lambda}{2},-\frac{\sqrt{3}\lambda}{4}\}$. These points verify that $\omega_\phi=-\frac{1}{3}$ and $q=0$. These points describe a universe dominated by the Gauss-Bonnet term. Using a strategy similar to that shown in Sec. IV A that is, re-scaling the system dividing by $\sqrt{1-\rho^2}$, we obtain that the stability of points $Q_{5,6}$ is given by the eigenvalues $\{\pm2,-\frac{\sqrt{3}\lambda}{2},-\frac{\sqrt{3}\lambda}{4}\}$.
   (a) Q_5 is a source (Q_6 is a saddle) for $\lambda<0$,
   (b) Q_5 is a saddle (Q_6 is a sink) for $\lambda>0$, and
   (c) they are nonhyperbolic for $\lambda=0$.

(4) $Q_{7,8}=(1,\frac{3\pi}{4},\pm1)$, with eigenvalues $\{0,\frac{\sqrt{3}\lambda}{4},\frac{\sqrt{3}\lambda}{2}\}$. These points verify that $\omega_\phi=-\frac{1}{3}$ and $q=0$. These points describe a universe dominated by the Gauss-Bonnet term. Using a strategy similar to that shown in Sec. IV A that is, re-scaling the system dividing by $\sqrt{1-\rho^2}$, we obtain that the stability of the points $Q_{5,6}$ is given by the eigenvalues $\{\pm2,\frac{\sqrt{3}\lambda}{2},\frac{\sqrt{3}\lambda}{4}\}$.

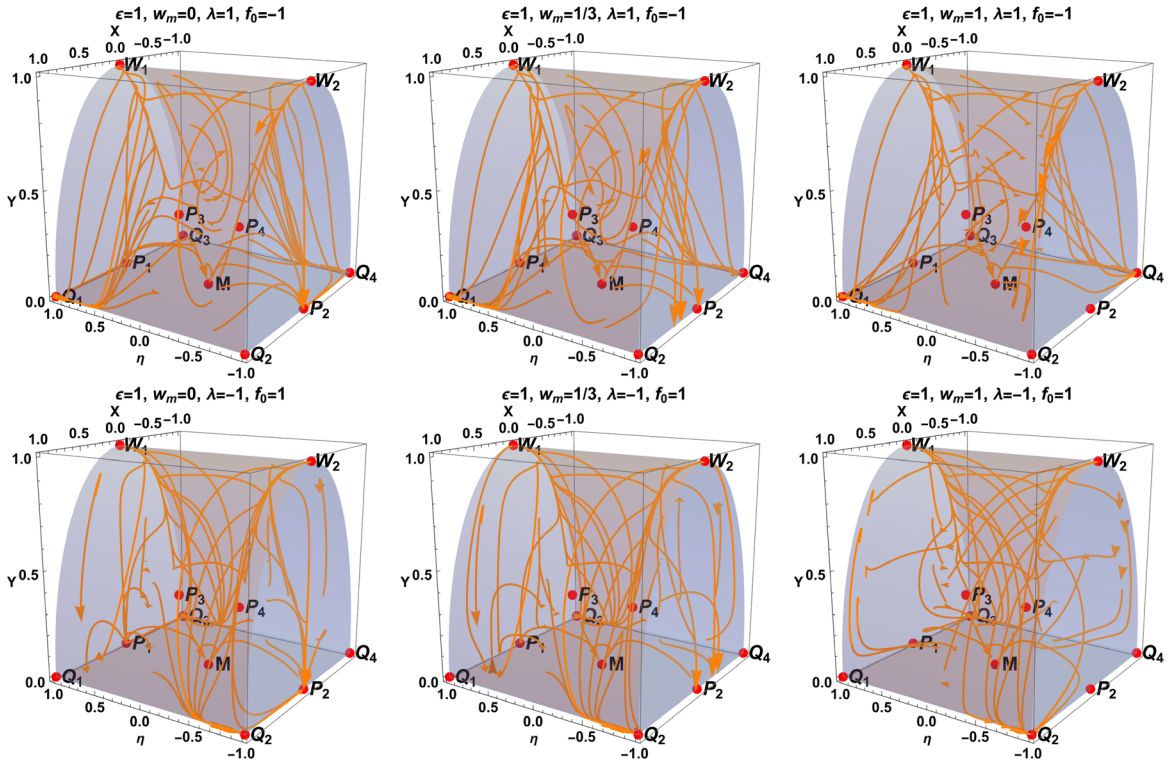

FIG. 5. Phase-space analysis for system (25)–(27) for $\epsilon = 1$ and different values of the parameters λ, f_0. Here we consider $Y > 0$ and the three cases $w_m = 0, \frac{1}{3}, 1$. The points $W_{1,2}$ are singularities where both the numerator and denominator of the equations of the system vanish.

(a) Q_7 is a source (Q_8 is a saddle) for $\lambda > 0$,
(b) Q_7 is a saddle (Q_8 is a sink) for $\lambda < 0$, and
(c) they are nonhyperbolic for $\lambda = 0$.

(5) $Q_{9,10} = \left(1, \frac{\pi}{4}, \pm\frac{1}{\sqrt{1-4f_0\lambda}}\right)$, with eigenvalues $\{-\frac{\sqrt{3}\lambda}{2}, -\sqrt{3}\lambda, -\sqrt{3}\lambda\}$. These points verify that $\omega_\phi = w_m - \frac{4}{3}$ and $q = \frac{3(w_m-1)}{2}$, in Fig. 6 we see the plot of these observables and note for instance that: for $w_m = 0$ the values are $\omega_\phi = -\frac{4}{3}$, $q = -\frac{3}{2}$; for $w_m = \frac{1}{3}$ the values are $\omega_\phi = -1$, $q = -1$ that is, they are de Sitter points; for $w_m = 1$ the values are $\omega_\phi = -\frac{1}{3}$, $q =$ that is, they are Gauss-Bonnet points. These points are
(a) sources for $\lambda < 0$,
(b) sinks for $\lambda > 0$, and
(c) nonhyperbolic for $\lambda = 0$.

(6) $Q_{11,12} = \left(1, \frac{3\pi}{4}, \pm\frac{1}{\sqrt{1-4f_0\lambda}}\right)$, with eigenvalues $\{\frac{\sqrt{3}\lambda}{2}, \sqrt{3}\lambda, \sqrt{3}\lambda\}$. These points also verify that $\omega_\phi = w_m - \frac{4}{3}$ and $q = \frac{3(w_m-1)}{2}$, again in Fig. 6 we see the plot of these observables this means that the interpretation is the same as in the previous points. These points are
(a) sources for $\lambda > 0$,
(b) sinks for $\lambda < 0$, and
(c) nonhyperbolic for $\lambda = 0$.

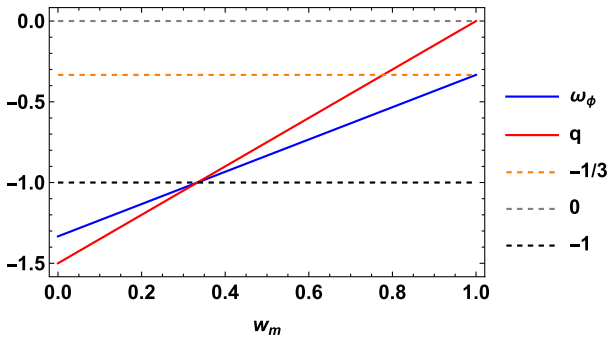

FIG. 6. Plot of ω_ϕ and q where we set $w_m \in [0, 1]$.

Figure 7 shows a phase-space analysis for system (25)–(27) for $\epsilon = -1$ and different values of the parameters λ, f_0. Here we consider $Y > 0$ and the two cases $w_m = 0$ (dust) and $\frac{1}{3}$ (radiation). The points $W_{1,2}$ are singularities where both the numerator and denominator of the equations of the system vanish.

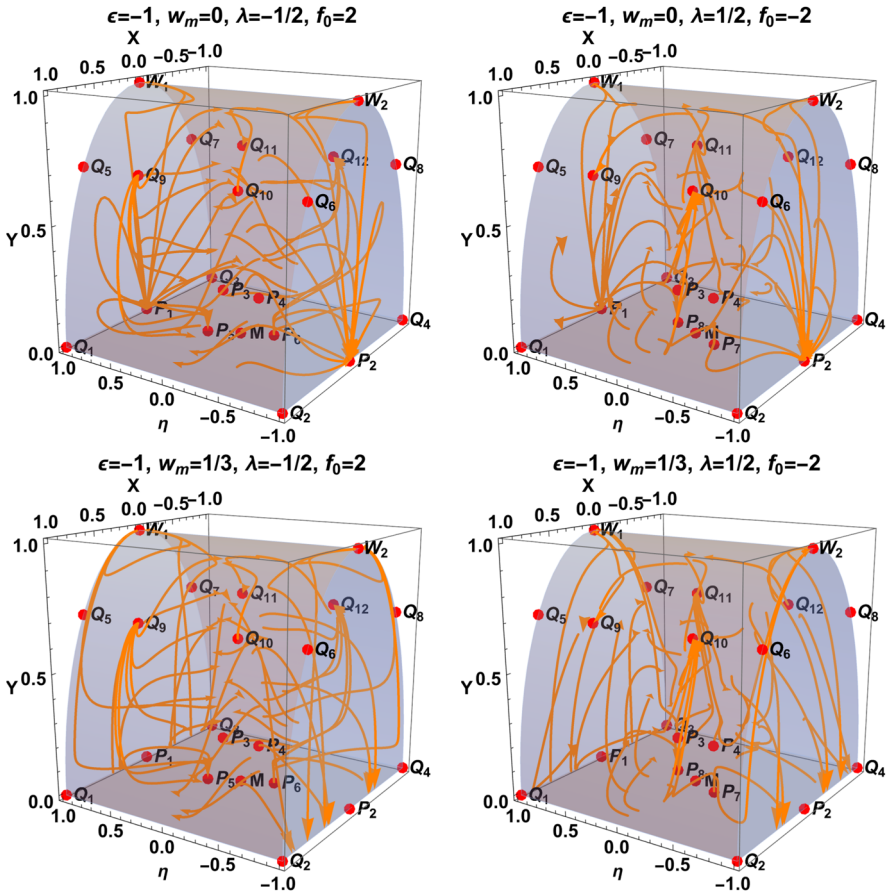

FIG. 7. Phase-space analysis for system (25)–(27) for $\epsilon=-1$ and different values of the parameters λ, f_0. Here we consider $Y>0$ and the two cases $w_m=0,\frac{1}{3}$. The points $W_{1,2}$ are singularities where both the numerator and denominator of the equations of the system vanish.

V. DYNAMICAL SYSTEM ANALYSIS FOR: $y=0$, $\lambda=0$

In this section, we study the case where the model has no scalar field potential, equivalent to setting $\lambda=y=0$ in system (20)–(22). With these assumptions, we have a reduced 2-dimensional system given by

$$\frac{dx}{d\tau}=\frac{1}{K}[\eta(3x(\eta^6(64f_0^2+w_m\epsilon+\epsilon)-2\eta^4(96f_0^2w_m+(w_m+2)\epsilon)+(w_m+5)\epsilon\eta^2-2\epsilon))+\eta(-4\sqrt{6}f_0(3w_m+1)\eta^3(\eta^2-1)+4\sqrt{6}f_0\epsilon\eta(\eta^2-1)x^2((6w_m-2)\eta^2+3(w_m-5))-3(w_m-1)(\eta^2-1)^2x^3)], \quad (35)$$

$$\frac{d\eta}{d\tau}=\frac{1}{K}[(\eta^2-1)(192f_0^2\eta^6+8\sqrt{6}f_0(3w_m-1)\epsilon(\eta^2-1)\eta^3x+3\epsilon(\eta^2-1)^2((w_m+1)\eta^2+x^2(\epsilon-w_m\epsilon)))]. \quad (36)$$

A. Dynamical analysis for $\epsilon=1$

The equilibrium points for system (35) and (36) in the coordinates (x,η) are the following.

(1) $M=(0,0)$, with eigenvalues $\{0,0\}$. The asymptotic solution is that of the Minkowski spacetime.

(2) $P_{1,2}=(0,\pm1)$, with eigenvalues $\{\pm2,\pm(1-3w_m)\}$. The asymptotic solution described by $P_{1,2}$ is a universe dominated by the Gauss-Bonnet term. We also verify that $\omega_\phi=-\frac{1}{3}$, and $q=0$. These points are
   (a) P_1 is a source (P_2 is a sink) for $0\le w_m<\frac{1}{3}$,
   (b) saddles for $\frac{1}{3}<w_m\le 1$, and
   (c) nonhyperbolic for $w_m=\frac{1}{3}$.

In Fig. 8 we present a phase portrait of system (35) and (36) for $\epsilon=1$, for the three values $w_m=0$ (dust), $\frac{1}{3}$ (radiation) and 1 (stiff matter). A summary of the analysis performed in this section is given in Table III.

B. Dynamical analysis for $\epsilon=-1$

The equilibrium points of system (35) and (36) for $\epsilon=-1$ in the coordinates (x,y) are the same as in the previous section plus some additional points, the complete list is the following

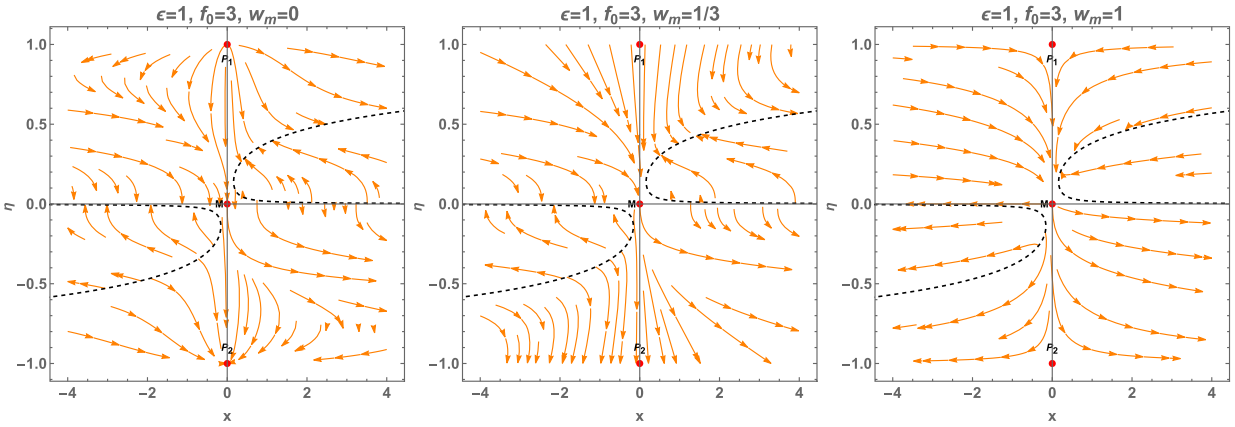

FIG. 8. Phase portrait for (35) and (36) for $\epsilon = 1$, for $w_m = 0, \frac{1}{3}, 1$. The black-dashed lines correspond to the values where $K = 0$, which corresponds to singular curves where the flow direction and the stability change.

(1) $M = (0, 0)$, with eigenvalues $\{0, 0\}$. This is a Minkowski point, and the analysis is the same as in Sec. V A.

(2) $P_1 = (0, \pm 1)$, with eigenvalues $\{\pm 2, \pm(1 - 3w_m)\}$. These are Gauss-Bonnet points; the analysis is the same as in Sec. V A.

(3) $P_3 = \left(\frac{1}{\sqrt{20\sqrt{\frac{10}{3}}f_0+5}}, \frac{\sqrt{3}}{\sqrt{4\sqrt{30}f_0+3}}\right)$, with eigenvalues $\left\{-\frac{3(w_m+1)}{\sqrt{4\sqrt{\frac{10}{3}}f_0+1}}, -\frac{9(4\sqrt{10}f_0+\sqrt{3})}{(4\sqrt{30}f_0+3)^{3/2}}\right\}$. This point exists for $f_0 \geq 0$ and it describes a de Sitter universe since $\omega_\phi = -1$ and $q = -1$. This point is a sink for all $f_0 \geq 0$ and $w_m \in [0, 1]$.

(4) $P_4 = \left(-\frac{1}{\sqrt{20\sqrt{\frac{10}{3}}f_0+5}}, -\frac{\sqrt{3}}{\sqrt{4\sqrt{30}f_0+3}}\right)$, with eigenvalues $\left\{\frac{3(w_m+1)}{\sqrt{4\sqrt{\frac{10}{3}}f_0+1}}, \frac{9(4\sqrt{10}f_0+\sqrt{3})}{(4\sqrt{30}f_0+3)^{3/2}}\right\}$. This point exists for $f_0 \geq 0$ and it describes a de Sitter universe since $\omega_\phi = -1$ and $q = -1$. This point is a source for all $f_0 \geq 0$ and $w_m \in [0, 1]$.

(5) $P_5 = \left(\frac{1}{\sqrt{5-20\sqrt{\frac{10}{3}}f_0}}, -\frac{\sqrt{3}}{\sqrt{3-4\sqrt{30}f_0}}\right)$, with eigenvalues $\left\{\frac{9(\sqrt{(\sqrt{3}-4\sqrt{10}f_0)^2}w_m-4\sqrt{10}f_0(w_m+2)+\sqrt{3}(w_m+2))}{2(3-4\sqrt{30}f_0)^{3/2}}, -\frac{9\sqrt{(\sqrt{3}-4\sqrt{10}f_0)^2}w_m+36\sqrt{10}f_0(w_m+2)-9\sqrt{3}(w_m+2)}{2(3-4\sqrt{30}f_0)^{3/2}}\right\}$. This point exists for $f_0 \leq 0$ and it describes a de Sitter universe since $\omega_\phi = -1$ and $q = -1$. This point is a source for all $f_0 \leq 0$ and $w_m \in [0, 1]$.

(6) $P_6 = \left(-\frac{1}{\sqrt{5-20\sqrt{\frac{10}{3}}f_0}}, \frac{\sqrt{3}}{\sqrt{3-4\sqrt{30}f_0}}\right)$, with eigenvalues $\left\{\frac{9\sqrt{(\sqrt{3}-4\sqrt{10}f_0)^2}w_m+36\sqrt{10}f_0(w_m+2)-9\sqrt{3}(w_m+2)}{2(3-4\sqrt{30}f_0)^{3/2}}, -\frac{9(\sqrt{(\sqrt{3}-4\sqrt{10}f_0)^2}w_m-4\sqrt{10}f_0(w_m+2)+\sqrt{3}(w_m+2))}{2(3-4\sqrt{30}f_0)^{3/2}}\right\}$. This point exists for $f_0 \leq 0$ and it describes a de Sitter universe since $\omega_\phi = -1$ and $q = -1$. This point is a sink for all $f_0 \leq 0$ and $w_m \in [0, 1]$.

In Fig. 9, we present different phase portraits for system (35) and (36) for $\epsilon = -1$ with two configurations: in the top row, we fix $f_0 = 3$ to show points $P_{3,4}$; we also show $P_{5,6}$ by setting $f_0 = -3$ in the bottom row. The values for the EoS parameter used for the plots are $w_m = 0$ (dust), $\frac{1}{3}$ (radiation), and 1 (stiff matter). A summary of the analysis of this section is presented in Table IV.

C. Infinity analysis for system (35) and (36) for $\epsilon = 1$

The numerical results in Secs. V A–V B suggest nontrivial dynamics when $x \to \pm\infty$. For that reason, we introduce the compacted variable

TABLE III. Equilibrium points of system (35) and (36) for $\epsilon = +1$ with their stability conditions. Also includes the value of ω_ϕ and q.

Label	x	η	Stability	ω_ϕ	q
M	0	0	Nonhyperbolic	Indeterminate	Indeterminate
P_1	0	1	Source for $0 \leq w_m < 1/3$		
			Saddle for $1/3 < w_m \leq 1$		
			Nonhyperbolic for $w_m = 1/3$	$-\frac{1}{3}$	0
P_2	0	-1	Sink for $0 \leq w_m < 1/3$		
			Saddle for $1/3 < w_m \leq 1$		
			Nonhyperbolic for $w_m = 1/3$	$-\frac{1}{3}$	0

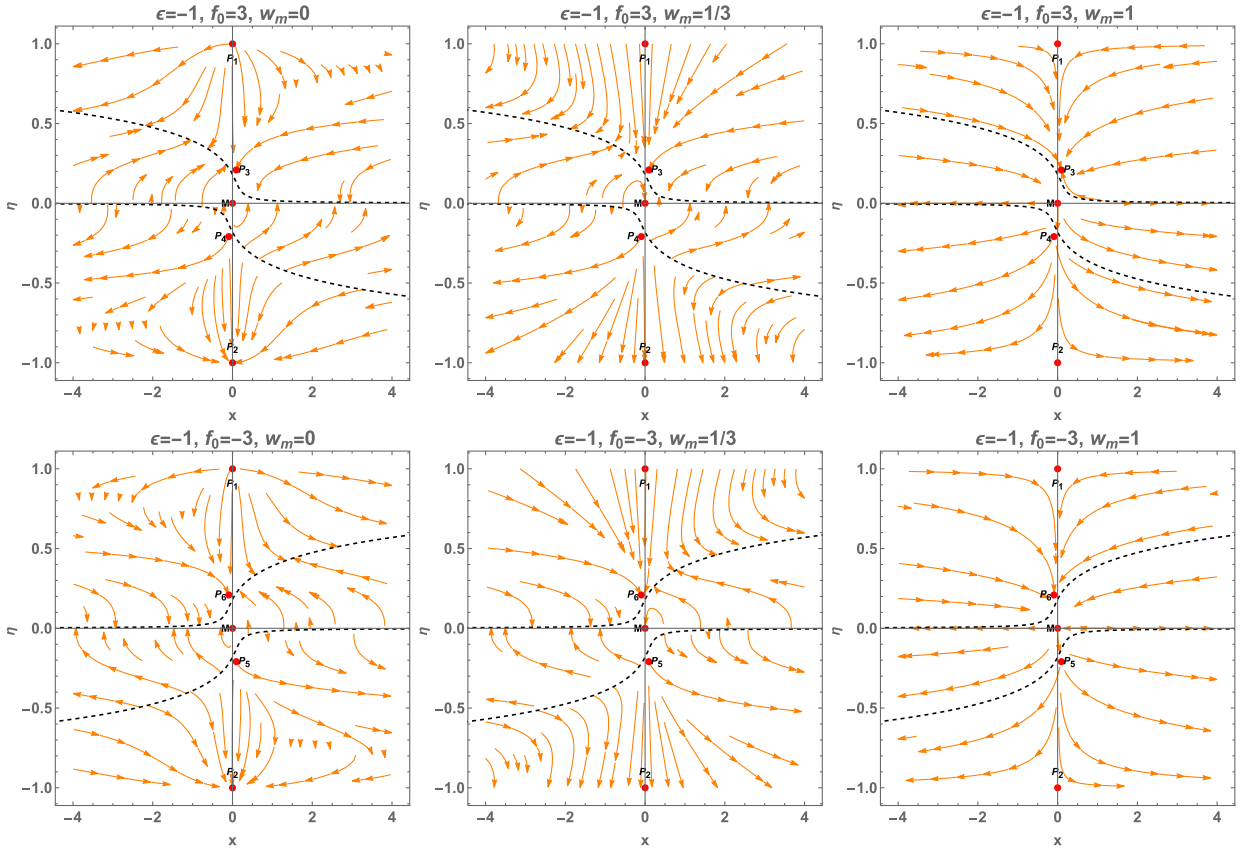

FIG. 9. Phase portrait for (35) and (36) for $\epsilon = -1$, for $w_m = 0, \frac{1}{3}, 1$ and $f_0 = \pm 3$. The black-dashed lines correspond to the values where $K = 0$, which corresponds to singular curves where the flow direction and the stability change.

$$u = \frac{x}{\sqrt{1+x^2}}, \tag{37}$$

with inverse

$$x = \frac{u}{\sqrt{1-u^2}}, \tag{38}$$

and the new time variable

$$f' = \sqrt{1-u^2}\frac{df}{d\tau}. \tag{39}$$

Note that for $u \to \pm 1$ we have dynamics for $x \to \infty$.

Using the compacted variable (37) together with system (35) and (36) we obtain the following compacted dynamical system

TABLE IV. Equilibrium points of system (35) and (36) for $\epsilon = -1$ with their stability conditions. Also includes the value of ω_ϕ and q.

Label	x	η	Stability	ω_ϕ	q
M	0	0	Nonhyperbolic	Indeterminate	Indeterminate
P_1	0	1	Source for $0 \le w_m < 1/3$		
			Saddle for $1/3 < w_m \le 1$		
			Nonhyperbolic for $w_m = 1/3$	$-\frac{1}{3}$	0
P_2	0	-1	Sink for $0 \le w_m < 1/3$		
			Saddle for $1/3 < w_m \le 1$		
			Nonhyperbolic for $w_m = 1/3$	$-\frac{1}{3}$	0
P_3	$\frac{1}{\sqrt{20\sqrt{\frac{10}{3}}f_0+5}}$	$\frac{\sqrt{3}}{\sqrt{4\sqrt{30}f_0+3}}$	Sink	-1	-1
P_4	$-\frac{1}{\sqrt{20\sqrt{\frac{10}{3}}f_0+5}}$	$-\frac{\sqrt{3}}{\sqrt{4\sqrt{30}f_0+3}}$	Source	-1	-1
P_5	$\frac{1}{\sqrt{5-20\sqrt{\frac{10}{3}}f_0}}$	$-\frac{\sqrt{3}}{\sqrt{3-4\sqrt{30}f_0}}$	Source	-1	-1
P_6	$-\frac{1}{\sqrt{5-20\sqrt{\frac{10}{3}}f_0}}$	$\frac{\sqrt{3}}{\sqrt{3-4\sqrt{30}f_0}}$	Sink	-1	-1

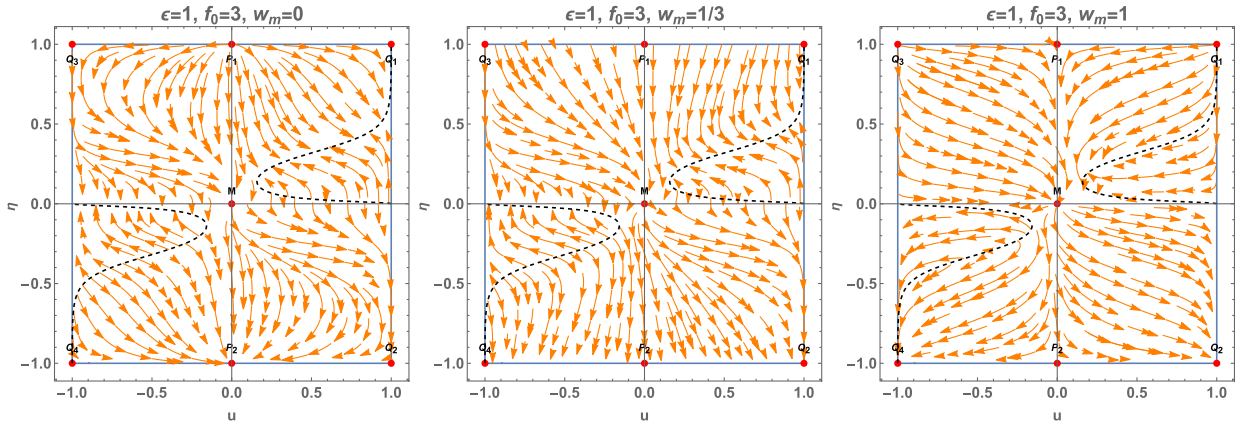

FIG. 10. Phase-plot analysis for system (40) and (41) for $\epsilon = 1$ and $f_0 = 3$. We also consider the cases $w_m = 0, \frac{1}{3}, 1$. The dashed black lines correspond to singularities where the flow changes direction.

$$
\begin{aligned}
u' = \frac{\eta(1-u^2)}{K_1}\{&3(1-u^2)u(64f_0^2\eta^4(\eta^2-3w_m)\\
&+(\eta^2-1)^2\epsilon(\eta^2(w_m+1)-2))\\
&-4\sqrt{6}f_0\eta^3(\eta^2-1)(1-u^2)^{3/2}(3w_m+1)\\
&+4f_0\eta(\eta^2-1)\sqrt{6-6u^2}u^2\epsilon(\eta^2(6w_m-2)\\
&+3(w_m-5))-3(\eta^2-1)^2u^3(w_m-1)\},
\end{aligned}
\tag{40}
$$

$$
\begin{aligned}
\eta' = \frac{(\eta^2-1)}{K_1}\{&3\eta^2(1-u^2)(64f_0^2\eta^4+(\eta^2-1)^2(w_m+1)\epsilon)\\
&+8f_0(\eta^2-1)\eta^3u\sqrt{6-6u^2}(3w_m-1)\epsilon\\
&-3(\eta^2-1)^2u^2(w_m-1)\},
\end{aligned}
\tag{41}
$$

where $K_1 := K_1(u,\eta,\epsilon,f_0) = 2(\sqrt{1-u^2}(96f_0^2\eta^4 + (\eta^2-1)^2\epsilon) + 8\sqrt{6}f_0\eta(\eta^2-1)u\epsilon)$.

Setting $\epsilon = 1$ in system (40) and (41) and rescaling the system dividing by $\sqrt{1-u^2}$, the equilibrium points are the same ones as in Sec. V A plus new points at infinity that satisfy $u = \pm 1$. We present first the new points followed by the points from the finite regime.

(1) $Q_{1,2} = (1, \pm 1)$, with eigenvalues $\{\pm 2, \pm 2(3w_m - 1)\}$. These points describe a universe dominated by the Gauss-Bonnet term; we also verify that $\omega_\phi = -\frac{1}{3}$ and $q = 0$. These points are
   (a) Q_1 is a source (Q_2 is a sink) for $\frac{1}{3} < w_m \leq 1$,
   (b) a saddle for $0 \leq w_m < \frac{1}{3}$, and
   (c) nonhyperbolic for $w_m = \frac{1}{3}$.

(2) $Q_{3,4} = (-1, \pm 1)$, with eigenvalues $\{\pm 2, \pm 2(3w_m - 1)\}$. These are Gauss-Bonnet points; the analysis is the same as Q_1 and Q_2, respectively.

(3) $M = (0, 0)$, see Sec. V A.

(4) $P_1 = (0, 1)$, see Sec. V A.

(5) $P_2 = (0, -1)$, see Sec. V A.

In Fig. 10, we present various phase portraits for system (40) and (41) for $\epsilon = 1$ and different values of the EoS parameter $w_m = 0$ (dust), $\frac{1}{3}$ (radiation) and 1 (stiff matter). These plots contain the finite regime points M and P_i and the infinite regime points Q_i. In Table V, we present a summary of the stability analysis only for the points on the infinite regime; this table can be complemented with the information from Table III.

D. Infinity analysis for system (35) and (36) for $\epsilon = -1$

Setting $\epsilon = -1$ in system (40) and (41), the equilibrium points are the same ones as in Sec. V B plus new points at infinity that satisfy $u = \pm 1$. As before, we present first the new points followed by the points from the finite regime.

(1) $Q_{1,2} = (1, \pm 1)$, with eigenvalues $\{\pm 2, \pm 2(3w_m - 1)\}$. These points are Gauss-Bonnet points, and the analysis is the same as in Sec. V C.

(2) $Q_{3,4} = (-1, \pm 1)$, with eigenvalues $\{\pm 2, \pm 2(3w_m - 1)\}$. These points are Gauss-Bonnet points, and the analysis is the same as in Sec. V C.

(3) $M = (0, 0)$, see Sec. V A.

(4) $P_1 = (0, 1)$, see Sec. V A.

TABLE V. Equilibrium points of system (40) and (41) for $\epsilon = \pm 1$ with their stability conditions. Also includes the value of ω_ϕ and q.

Label	x	η	Stability	ω_ϕ	q
Q_1	1	1	Saddle for $0 \leq w_m < 1/3$		
			Source for $1/3 < w_m \leq 1$		
			Nonhyperbolic for $w_m = 1/3$	$-\frac{1}{3}$	0
Q_2	1	-1	Saddle for $0 \leq w_m < 1/3$		
			Sink for $1/3 < w_m \leq 1$		
			Nonhyperbolic for $w_m = 1/3$	$-\frac{1}{3}$	0
Q_3	-1	1	Saddle for $0 \leq w_m < 1/3$		
			Source for $1/3 < w_m \leq 1$		
			Nonhyperbolic for $w_m = 1/3$	$-\frac{1}{3}$	0
Q_4	-1	-1	Saddle for $0 \leq w_m < 1/3$		
			Sink for $1/3 < w_m \leq 1$		
			Nonhyperbolic for $w_m = 1/3$	$-\frac{1}{3}$	0

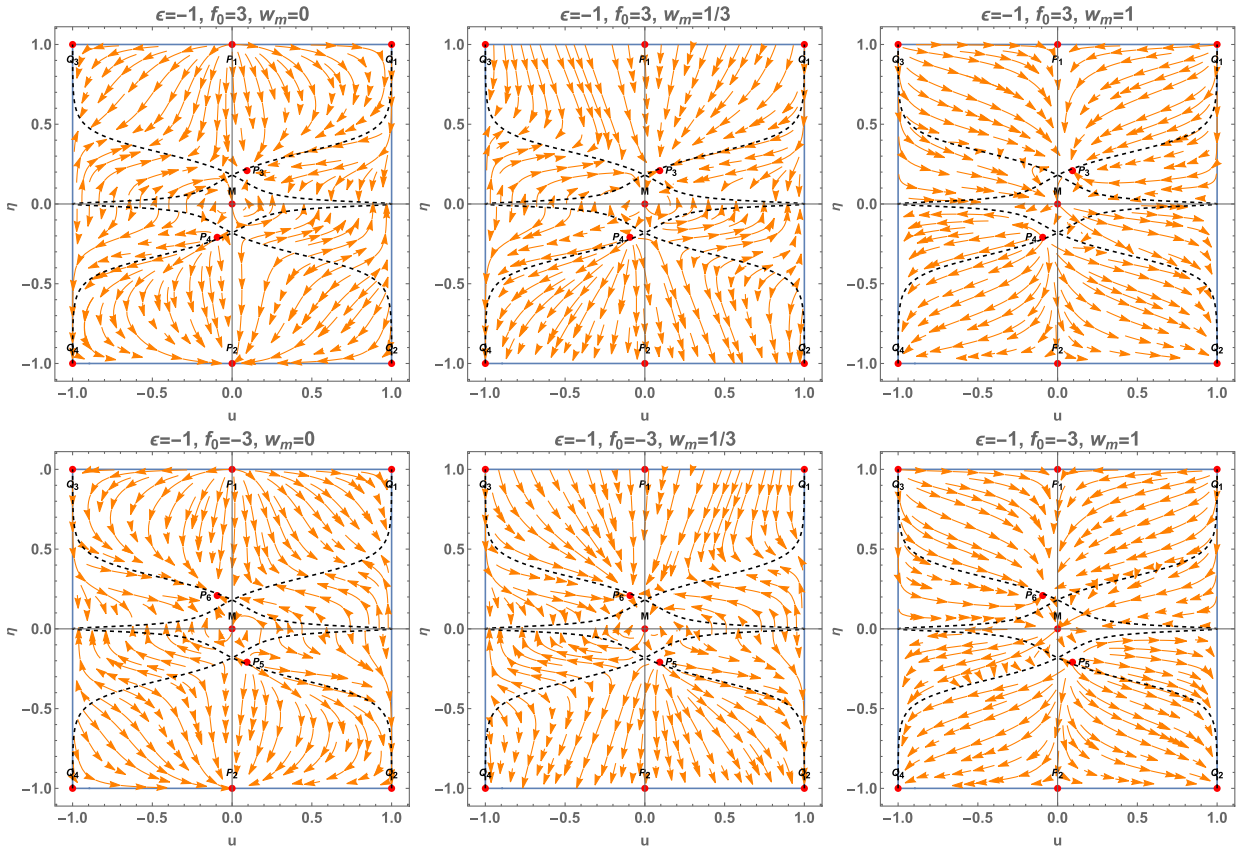

FIG. 11. Phase-plot analysis for system (40) and (41) for $\epsilon = -1$ and $f_0 = 3$. We also consider the cases $w_m = 0, \frac{1}{3}, 1$. The dashed black lines correspond to singularities where the flow changes direction.

(5) $P_2 = (0, -1)$, see Sec. V A.
(6) $P_3 = \left(\frac{1}{\sqrt{20\sqrt{\frac{10}{3}}f_0+5}}, \frac{\sqrt{3}}{\sqrt{4\sqrt{30}f_0+3}}\right)$, see Sec. V B.
(7) $P_4 = \left(-\frac{1}{\sqrt{20\sqrt{\frac{10}{3}}f_0+5}}, -\frac{\sqrt{3}}{\sqrt{4\sqrt{30}f_0+3}}\right)$, see Sec. V B.
(8) $P_5 = (0, -1)$, see Sec. V B.
(9) $P_6 = (0, -1)$, see Sec. V B.

In Fig. 11, we present various phase portraits for system (40) and (41) for $\epsilon = -1$ different values of the EoS parameter $w_m = 0$ (dust), $\frac{1}{3}$ (radiation) and 1 (stiff matter). As before, we set two values for f_0 to show the points $P_{3,4}$ and $P_{5,6}$. These plots contain the finite regime points M and P_i as well as the infinite regime points Q_i. Note that the infinite regime points are the same for both values of ϵ; therefore, we present the summary of the stability analysis in Table V once again, but in this case, the information can be complemented with Table IV.

VI. CONCLUSIONS

In this paper, we have extended our previous study [46] by introducing an ideal gas which can describe the radiation, dark matter, or dark energy, depending on the equation of state, in the Einstein-Gauss-Bonnet scalar field model in a four-dimensional cosmology. In addition, we performed a detailed analysis of the phase space and reconstructed the asymptotic behavior of the physical parameters.

New dimensionless variables different from that of the H-normalization have been introduced. We wrote the field equations in the equivalent form of a four-dimensional algebraic-differential system of first-order equations. Because of the algebraic constraint, the dimension of the latter system is reduced to three. Moreover, for $\rho_m = 0$, we recover the two-dimensional system investigated in [46].

We determined the equilibrium points for the field equations in the finite and infinite regimes. For the latter, we define a set of compact variables. Then, we calculated the asymptotic behavior of the physical parameters for each equilibrium point. For the linear coupling between the scalar field and the Gauss-Bonnet component, asymptotic solutions exist that describe the de Sitter spacetime or a universe dominated by the Gauss-Bonnet scalar.

We have shown that the stability properties of the equilibrium points depend on the nature of the ideal gas (its equation of state parameter), the scalar field and the scalar f_0 of the coupling function for the Gauss-Bonnet term.

For the general case described in Sec. III B with $\epsilon = 1$ we obtained the following results: the Gauss-Bonnet point P_1 is a source for $0 \leq w_m < \frac{1}{3}$; the Gauss-Bonnet point P_2 is

a sink for $0 \leq w_m < \frac{1}{3}$. For the general case described in Sec. III C with $\epsilon = -1$ we obtained the following results: the Gauss-Bonnet point P_1 is a source for $0 \leq w_m < \frac{1}{3}$; the Gauss-Bonnet point P_2 is a sink for $0 \leq w_m < \frac{1}{3}$; the de Sitter point P_3 is a sink for $f_0 < 0$ and $0 < \lambda < \sqrt{\frac{2}{3}}$; the de Sitter point P_4 is a source for $f_0 < 0$ and $0 < \lambda < \sqrt{\frac{2}{3}}$; the de Sitter point P_5 is a sink for $f_0 \geq 0$ and $\lambda < 0$; the de Sitter point P_6 is a source for $f_0 \geq 0$ and $\lambda < 0$; the de Sitter point P_7 is a source for $f_0 \leq 0$ and $\lambda > 0$; the de Sitter point P_8 is a sink for $f_0 \leq 0$ and $\lambda > 0$;

The numerical results suggested that there must be nontrivial dynamics at infinity; given this, in Sec. IV A, we investigated the infinity behavior for $\epsilon = 1$ and obtained the following results: the Gauss-Bonnet point Q_1 is a source for $\lambda > 0$ and $\frac{1}{3} < w_m \leq 1$; the Gauss-Bonnet point Q_2 is a sink for $\lambda > 0$ and $\frac{1}{3} < w_m \leq 1$; the Gauss-Bonnet point Q_3 is a source for $\lambda < 0$ and $\frac{1}{3} < w_m \leq 1$; the Gauss-Bonnet point Q_4 is a sink for $\lambda < 0$ and $\frac{1}{3} < w_m \leq 1$.

Similarly we obtained the following results for $\epsilon = -1$ in Sec. IV B for the behavior at infinity: the Gauss-Bonnet point Q_1 is a source for $\lambda > 0$ and $\frac{1}{3} < w_m \leq 1$; the Gauss-Bonnet point Q_2 is a sink for $\lambda > 0$ and $\frac{1}{3} < w_m \leq 1$; the Gauss-Bonnet point Q_3 is a source for $\lambda < 0$ and $\frac{1}{3} < w_m \leq 1$; the Gauss-Bonnet point Q_4 is a sink for $\lambda < 0$ and $\frac{1}{3} < w_m \leq 1$; the Gauss-Bonnet point Q_5 is a source for $\lambda < 0$; the Gauss-Bonnet point Q_6 is a sink for $\lambda > 0$; the Gauss-Bonnet point Q_7 is a source for $\lambda > 0$; the Gauss-Bonnet point Q_8 is a sink for $\lambda < 0$; the Gauss-Bonnet points $Q_{9,10}$ are sources for $\lambda < 0$ and sinks for $\lambda > 0$; the Gauss-Bonnet points $Q_{11,12}$ are sources for $\lambda > 0$ and sinks for $\lambda < 0$.

In Sec. V we study the case where $y = 0$ and $\lambda = 0$. There we studied a two-dimensional system for the variables x and η. Setting $\epsilon = 1$ in Sec. V A we obtained the following results: the Gauss-Bonnet point P_1 is a source for $0 \leq w_m < \frac{1}{3}$; the Gauss-Bonnet point P_2 is a sink for $0 \leq w_m < \frac{1}{3}$; On the other hand, setting $\epsilon = -1$ in Sec. V B we obtained the following results: the Gauss-Bonnet point P_1 is a source for $0 \leq w_m < \frac{1}{3}$; the Gauss-Bonnet point P_2 is a sink for $0 \leq w_m < \frac{1}{3}$; the de Sitter point P_3 is a sink for $f_0 \geq 0$ and $0 \leq w_m < 1$; the de Sitter point P_4 is a source for $f_0 \geq 0$ and $0 \leq w_m < 1$; the de Sitter point P_5 is a sink for $f_0 \leq 0$ and $0 \leq w_m < 1$; the de Sitter point P_6 is a sink for $f_0 \leq 0$ and $0 \leq w_m < 1$.

As in the general case, in Secs. V C and V D we investigated the behavior at infinity for the reduced system setting $\epsilon = \pm 1$ and obtained the following results: the Gauss-Bonnet point Q_1 is a source for $\frac{1}{3} < w_m \leq 1$; the Gauss-Bonnet point Q_2 is a sink for $\frac{1}{3} < w_m \leq 1$; the Gauss-Bonnet point Q_3 is a source for $\frac{1}{3} < w_m \leq 1$; the Gauss-Bonnet point Q_4 is a sink for $\frac{1}{3} < w_m \leq 1$.

Observe that when $x = y = 0$, we acquire $z = \eta^2$, which means $\Omega_m = \rho_m/(3H^2) = z/\eta^2 = 1$, and we have matter-dominated solutions. Accordingly, the gravitational models can admit a cosmological solution where the matter source dominates, $\Omega_m = 1$ (see Fig. 2).

For investigating the viability of the theory, it is desirable to have complete cosmological dynamics [72]; it should describe an early radiation-dominated era, later entering into an epoch of mater domination and finally reproducing the present acceleration of the Universe. In the dynamical systems language, complete cosmological dynamics can be understood as an orbit connecting a past attractor, also called a source, with a late-time attractor, also called a sink, that passes through some saddle points, such that radiation precedes matter domination. Some solutions interpolating between critical points can provide information on the intermediate stages of the evolution, with interest in orbits corresponding to a specific cosmological history [51,52].

To present one possible evolution of the physical model, Fig. 2 displays the expressions $\omega_\phi(\tau)$, $x(\tau)$, $y(\tau)$, and $\eta(\tau)$ evaluated at a solution of system (20)–(22) for $\epsilon = 1$ for the initial conditions for the left plot are $x(0) = 0.001, y(0) = \sqrt{\frac{\lambda}{\lambda - 8f_0}}, \eta(0) = -\sqrt{\frac{\lambda}{\lambda - 8f_0}}$. The solution is past asymptotic to $\omega_\phi = -1$ $(q = -1)$, then remains near the de Sitter point, then tending asymptotically to $\omega_\phi = -\frac{1}{3}$ (the Gauss-Bonnet point) from below. The initial conditions for the plot on the right are $x(0) = 0.001, y(0) = 0.001, \eta(0) = 0.9$. The solution is past asymptotic to $\omega_\phi = -\frac{1}{3}, q = 0$ (zero acceleration), then it grows to $\omega_\phi, q > 0$, finally, it tends asymptotically to $\omega_\phi = 0, q = \frac{1}{2}$ describing a matter-dominated solution.

In the same lines, Fig. 4 presents the expressions $\omega_\phi(\tau)$, $x(\tau)$, $y(\tau)$, and $\eta(\tau)$ evaluated at the solution of system (20)–(22) for $\epsilon = -1$. The initial conditions for the left plot are $x(0) = 0.001, y(0) = \sqrt{\frac{\lambda}{\lambda - 8f_0}}, \eta(0) = -\sqrt{\frac{\lambda}{\lambda - 8f_0}}$. The solution is past asymptotic to $\omega_\phi = -1$ $(q = -1)$, then remains near the de Sitter point, then tending asymptotically to $\omega_\phi = -\frac{1}{3}$ (the Gauss-Bonnet point) from below. The initial conditions for the plot on the right are $x(0) = 0.001, y(0) = 0.001, \eta(0) = 0.9$. The solution is past asymptotic to $\omega_\phi = -\frac{1}{3}$ (zero acceleration), then it tends asymptotically to a de Sitter phase $\omega_\phi = -1, q = -1$ describing a late-time acceleration.

Finally, one topic to be considered in further studies is reconstructing the cosmological history using different coupling functions between the scalar field and the Gauss-Bonnet scalar.

ACKNOWLEDGMENTS

A. D. M. was supported by Agencia Nacional de Investigación y Desarrollo (ANID) Subdirección de Capital Humano/Doctorado Nacional/año 2020 folio

21200837, Gastos operacionales Proyecto de tesis/2022 folio 242220121, and by Vicerrectoría de Investigación y Desarrollo Tecnológico (VRIDT) at Universidad Católica del Norte. G. L. was funded through Concurso De Pasantías De Investigación Año 2022, Resolución VRIDT No. 040/2022 and Resolución VRIDT No. 054/2022. Also, he was funded by Resolución VRIDT No. 026/2023 and Resolución VRIDT No. 027/2023. He also thanks the support of Núcleo de Investigación Geometría Diferencial y Aplicaciones, Resolución VRIDT N°096/2022, and A. P. acknowledges VRIDT-UCN through Concurso de Estadías de Investigación, Resolución VRIDT N°098/2022.

[1] A. Einstein, Ann. Phys. (Berlin) **49**, 769 (1916).
[2] D. Lovelock, Arch. Ration. Mech. Anal. **33**, 54 (1969).
[3] D. Lovelock, J. Math. Phys. (N.Y.) **12**, 498 (1971).
[4] C. M. Will, Living Rev. Relativity **17**, 4 (2014).
[5] B. P. Abbott *et al.* (LIGO Scientific and Virgo Collaborations), Phys. Rev. Lett. **116**, 061102 (2016).
[6] M. Kramer *et al.*, Phys. Rev. X **11**, 041050 (2021).
[7] A. G. Riess *et al.* (Supernova Search Team), Astron. J. **116**, 1009 (1998).
[8] M. Tegmark *et al.* (SDSS Collaboration), Astrophys. J. **606**, 702 (2004).
[9] A. H. Guth, Phys. Rev. D **23**, 347 (1981).
[10] A. D. Linde, Phys. Lett. **108B**, 389 (1982).
[11] J. D. Barrow, Phys. Rev. D **48**, 1585 (1993).
[12] B. Ratra and P. J. E. Peebles, Phys. Rev. D **37**, 3406 (1988).
[13] J. D. Barrow and P. Saich, Classical Quantum Gravity **10**, 279 (1993).
[14] D. F. Torres, Phys. Rev. D **66**, 043522 (2002).
[15] R. R. Caldwell, M. Kamionkowski, and N. N. Weinberg, Phys. Rev. Lett. **91**, 071301 (2003).
[16] M. C. Bento, O. Bertolami, and A. A. Sen, Phys. Rev. D **70**, 083519 (2004).
[17] S. Basilakos and G. Lukes-Gerakopoulos, Phys. Rev. D **78**, 083509 (2008).
[18] W. Liu, J. Ouyang, and H. Yang, Commun. Theor. Phys. **63**, 391 (2015).
[19] A. Kundu, S. D. Pathak, and V. K. Ojha, Commun. Theor. Phys. **73**, 025402 (2021).
[20] S. Capozziello, J. Matsumoto, S. Nojiri, and S. D. Odintsov, Phys. Lett. B **693**, 198 (2010).
[21] T. P. Sotiriou, Classical Quantum Gravity **23**, 5117 (2006).
[22] S. Nojiri, S. D. Odintsov, and V. K. Oikonomou, Phys. Rep. **692**, 1 (2017).
[23] T. Clifton, P. G. Ferreira, A. Padilla, and C. Skordis, Phys. Rep. **513**, 1 (2012).
[24] S. Nojiri, S. D. Odintsov, and M. Sasaki, Phys. Rev. D **71**, 123509 (2005).
[25] S. Nojiri, S. D. Odintsov, and M. Sami, Phys. Rev. D **74**, 046004 (2006).
[26] G. Cognola, E. Elizalde, S. Nojiri, S. Odintsov, and S. Zerbini, Phys. Rev. D **75**, 086002 (2007).
[27] S. Nojiri, S. D. Odintsov, and P. V. Tretyakov, Phys. Lett. B **651**, 224 (2007).
[28] T. Padmanabhan and D. Kothawala, Phys. Rep. **531**, 115 (2013).
[29] S. Nojiri and S. D. Odintsov, Phys. Rep. **505**, 59 (2011).
[30] S. D. Odintsov and V. K. Oikonomou, Phys. Rev. D **98**, 044039 (2018).
[31] S. D. Odintsov and V. K. Oikonomou, Phys. Lett. B **797**, 134874 (2019).
[32] S. D. Odintsov, V. K. Oikonomou, and F. P. Fronimos, Ann. Phys. (Amsterdam) **420**, 168250 (2020).
[33] S. D. Odintsov, V. K. Oikonomou, and F. P. Fronimos, Nucl. Phys. **B958**, 115135 (2020).
[34] D. Glavan and C. Lin, Phys. Rev. Lett. **124**, 081301 (2020).
[35] M. Gurses, T. c. Şişman, and B. Tekin, Phys. Rev. Lett. **125**, 149001 (2020).
[36] B. Li, J. D. Barrow, and D. F. Mota, Phys. Rev. D **76**, 044027 (2007).
[37] J. M. Armaleo, J. Osorio Morales, and O. Santillan, Eur. Phys. J. C **78**, 85 (2018).
[38] I. Fomin, Eur. Phys. J. C **80**, 1145 (2020).
[39] S. Nojiri, S. D. Odintsov, V. K. Oikonomou, and A. A. Popov, Nucl. Phys. **B973**, 115617 (2021).
[40] O. P. Santillan, J. Cosmol. Astropart. Phys. 07 (2017) 008.
[41] S. Chakraborty, T. Paul, and S. SenGupta, Phys. Rev. D **98**, 083539 (2018).
[42] I. V. Fomin, Phys. Part. Nucl. **49**, 525 (2018).
[43] R. A. Konoplya, T. Pappas, and A. Zhidenko, Phys. Rev. D **101**, 044054 (2020).
[44] N. Chatzarakis and V. K. Oikonomou, Ann. Phys. (Amsterdam) **419**, 168216 (2020).
[45] K. F. Dialektopoulos, J. Levi Said, and Z. Oikonomopoulou, arXiv:2211.06076.
[46] A. D. Millano, G. Leon, and A. Paliathanasis, Mathematics **11**, 1408 (2023).
[47] E. J. Copeland, A. R. Liddle, and D. Wands, Phys. Rev. D **57**, 4686 (1998).
[48] P. Kanti, R. Gannouji, and N. Dadhich, Phys. Rev. D **92**, 041302 (2015).
[49] P. Kanti, R. Gannouji, and N. Dadhich, Phys. Rev. D **92**, 083524 (2015).
[50] G. Hikmawan, J. Soda, A. Suroso, and F. P. Zen, Phys. Rev. D **93**, 068301 (2016).
[51] G. F. R. Ellis and J. Wainwright, *Dynamical Systems in Cosmology* (Cambridge University Press, Cambridge, England, 1997).
[52] A. A. Coley, *Dynamical Systems and Cosmology* (Kluwer, Dordrecht, Netherlands, 2003).

[53] L. Amendola, R. Gannouji, D. Polarski, and S. Tsujikawa, Phys. Rev. D **75**, 083504 (2007).
[54] A. A. Coley and R. J. van den Hoogen, Phys. Rev. D **62**, 023517 (2000).
[55] R. Lazkoz, G. Leon, and I. Quiros, Phys. Lett. B **649**, 103 (2007).
[56] C. Xu, E. N. Saridakis, and G. Leon, J. Cosmol. Astropart. Phys. 07 (2012) 005.
[57] B. Alhulaimi, A. Coley, and P. Sandin, J. Math. Phys. (N.Y.) **54**, 042503 (2013).
[58] G. Leon, E. González, A. D. Millano, and F. O. F. Silva, Classical Quantum Gravity **39**, 115003 (2022).
[59] A. Millano, Qualitative analysis of Einstein-aether models with perfect fluid and scalar fields, Master's thesis, Catolica del Norte University, 2020.
[60] G. Leon, A. Millano, and J. Latta, Eur. Phys. J. C **80**, 1192 (2020).
[61] G. Leon, E. González, S. Lepe, C. Michea, and A. D. Millano, Eur. Phys. J. C **81**, 414 (2021); **81**, 1097(E) (2021).
[62] G. Leon, E. González, S. Lepe, C. Michea, and A. D. Millano, Eur. Phys. J. C **81**, 867 (2021); **81**, 1096(E) (2021).
[63] G. Leon, S. Cuellar, E. Gonzalez, S. Lepe, C. Michea, and A. D. Millano, Eur. Phys. J. C **81**, 489 (2021); **81**, 1100(E) (2021).
[64] A. Hernández-Almada, G. Leon, J. Magaña, M. A. García-Aspeitia, V. Motta, E. N. Saridakis, K. Yesmakhanova, and A. D. Millano, Mon. Not. R. Astron. Soc. **512**, 5122 (2022).
[65] G. Leon, A. D. Millano, and A. Paliathanasis, Mathematics **11**, 120 (2023).
[66] B. Micolta-Riascos, A. D. Millano, G. Leon, C. Erices, and A. Paliathanasis, Fractal Fract. **7**, 149 (2023).
[67] A. D. Millano, K. Jusufi, and G. Leon, Phys. Lett. B **841**, 137916 (2023).
[68] A. D. Millano, G. Leon, and A. Paliathanasis, arXiv: 2304.08659.
[69] K. Jusufi, G. Leon, and A. D. Millano, arXiv:2304.11492.
[70] M. Cruz, A. Ganguly, R. Gannouji, G. Leon, and E. N. Saridakis, Classical Quantum Gravity **34**, 125014 (2017).
[71] V. K. Oikonomou, Phys. Rev. D **99**, 104042 (2019).
[72] A. Avelino, Y. Leyva, and L. A. Urena-Lopez, Phys. Rev. D **88**, 123004 (2013).